This slide intentionally left blank except for the message “This slide intentionally left blank except for the message

http://www.microscopy-uk.org.uk/index.html?http://www.microscopy-uk.org.uk/primer/history.htm

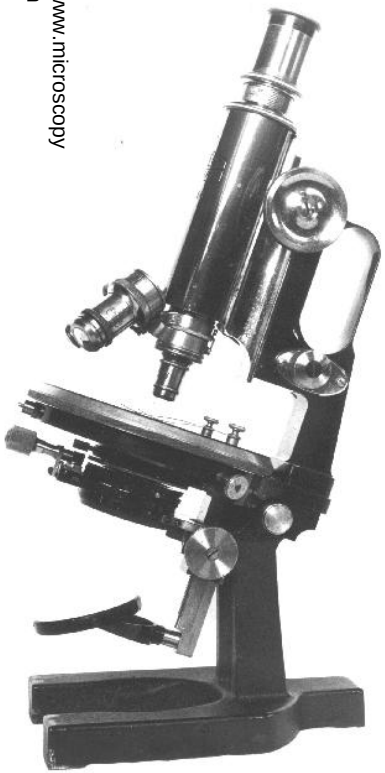

Fig. 9. Classic Zeiss stand, 1912

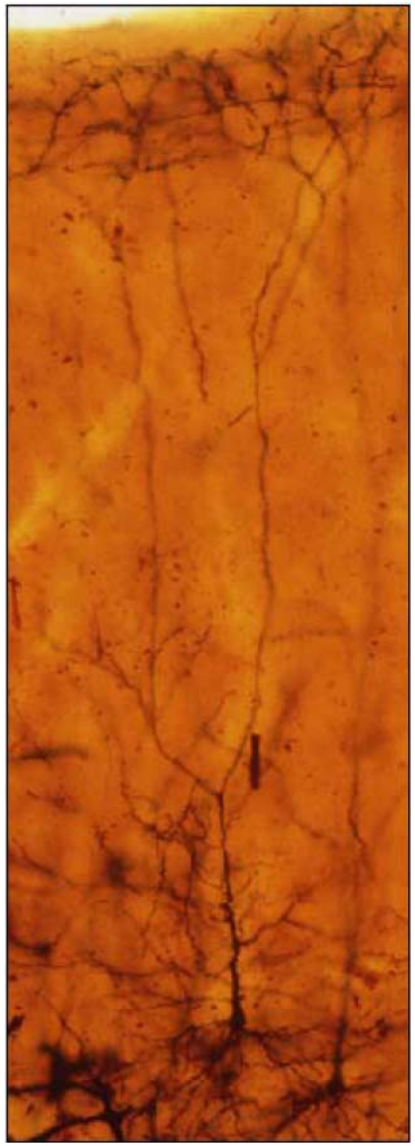

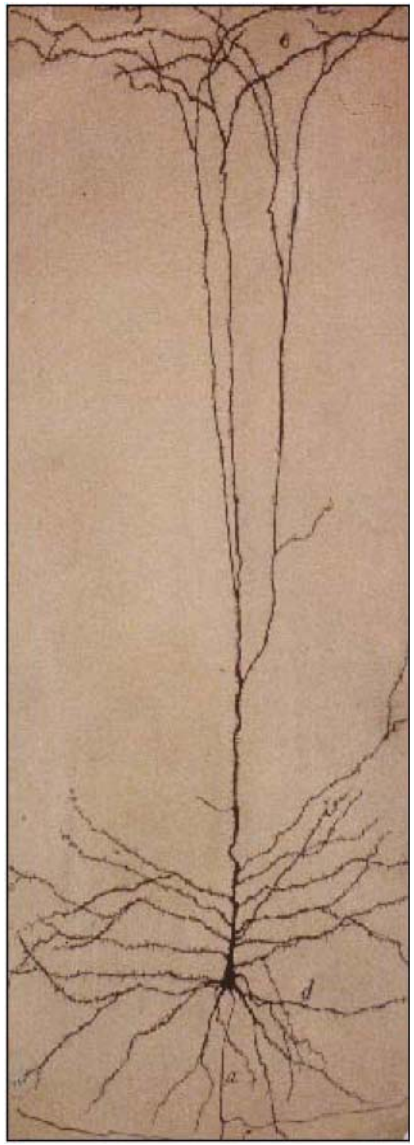

Photomicrograph from one of Cajal's Golgi preparations of the postcentral gyrus of a child showing a labeled pyramidal cell similar to the one shown in the left panel (from the collection of histological preparations housed in the Museo Cajal; published by DeFelipe and Jones, *Cajal on the Cerebral Cortex*. New York: Oxford University Press, 1988).*Right*, drawing by Cajal illustrating a Golgi-impregnated pyramidal neuron of the postcentral gyrus of achild published in 1899 (*Estudios sobre la corteza cerebral humana. II: Estructura de la corteza motriz del hombre y mamíferos superiores. Revista Trimestral Micrográfica* 4: 117-200). Left,

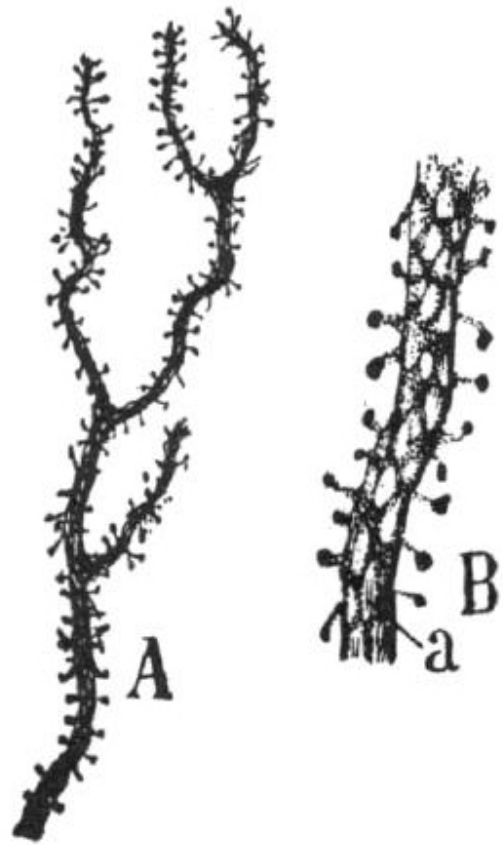

Low (A) and high (B) magnification views of dendritic spines from a cerebellar Purkinje cell, drawn by Cajal

(Ramón y Cajal, 1899).

http://ibronew.alp.mcgill.ca/Media/Images/si-how-den-figs-fig1.jpg

Figure 1.4. Professor Alexander Jabłoński (1898–1980), *circa* 1935. Courtesy of his daughter, Professor Danuta Frąckowiak.

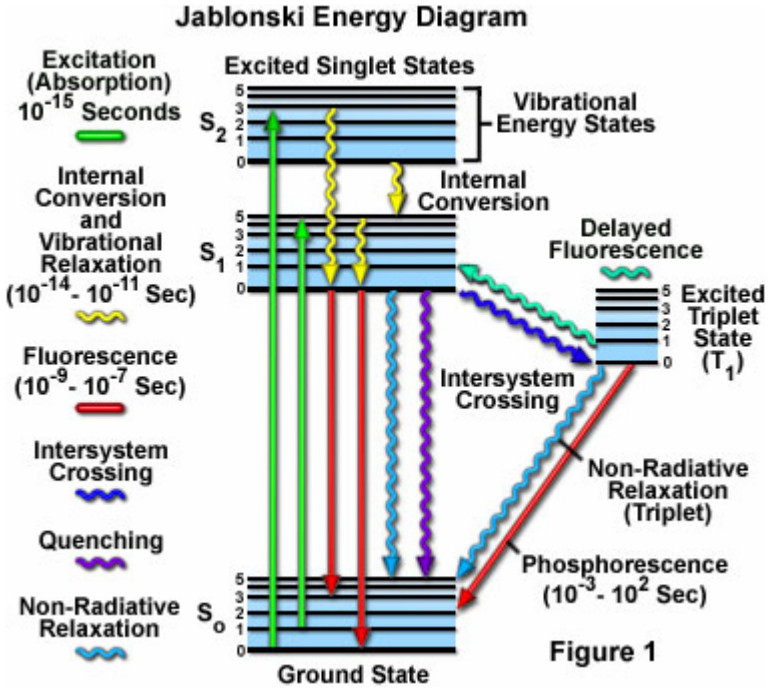

From: Lakowicz, Principles of Fluroescence Spectroscopy

http://micro.magnet.fsu.edu/optics/timeline/people/jablonski.html

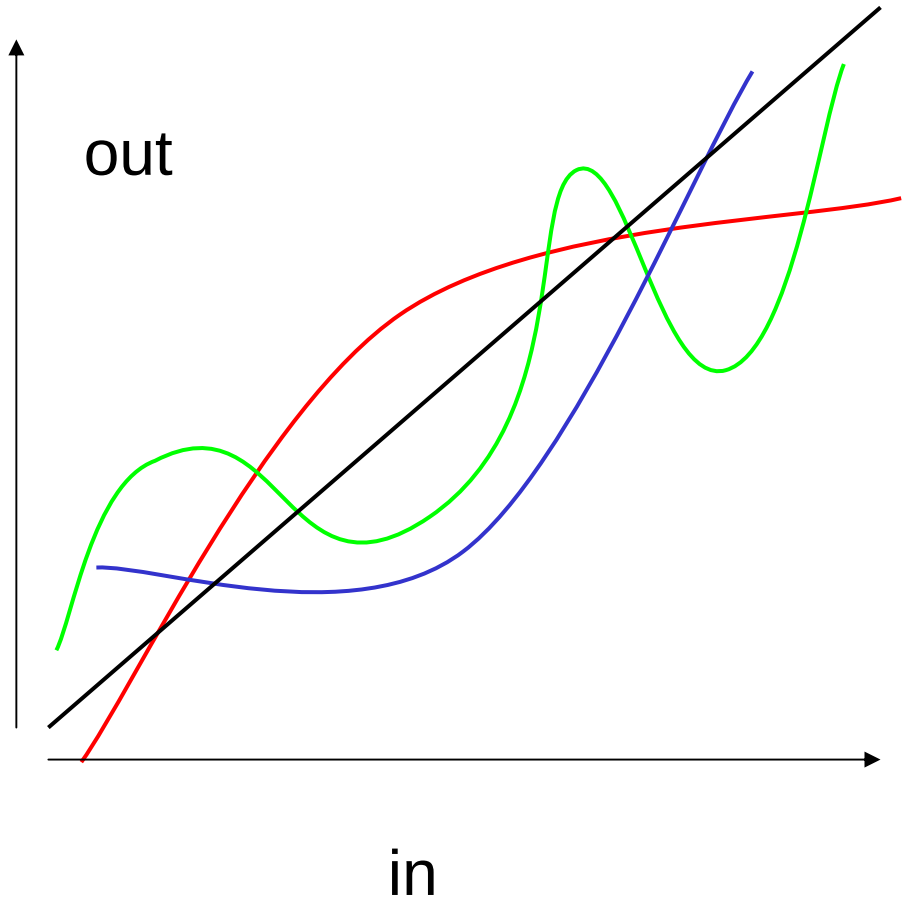

Linearity

$f(a + b) = f(a) + f(b)$

$f(\beta * a) = \beta * f(a)$

Superposition

Independence

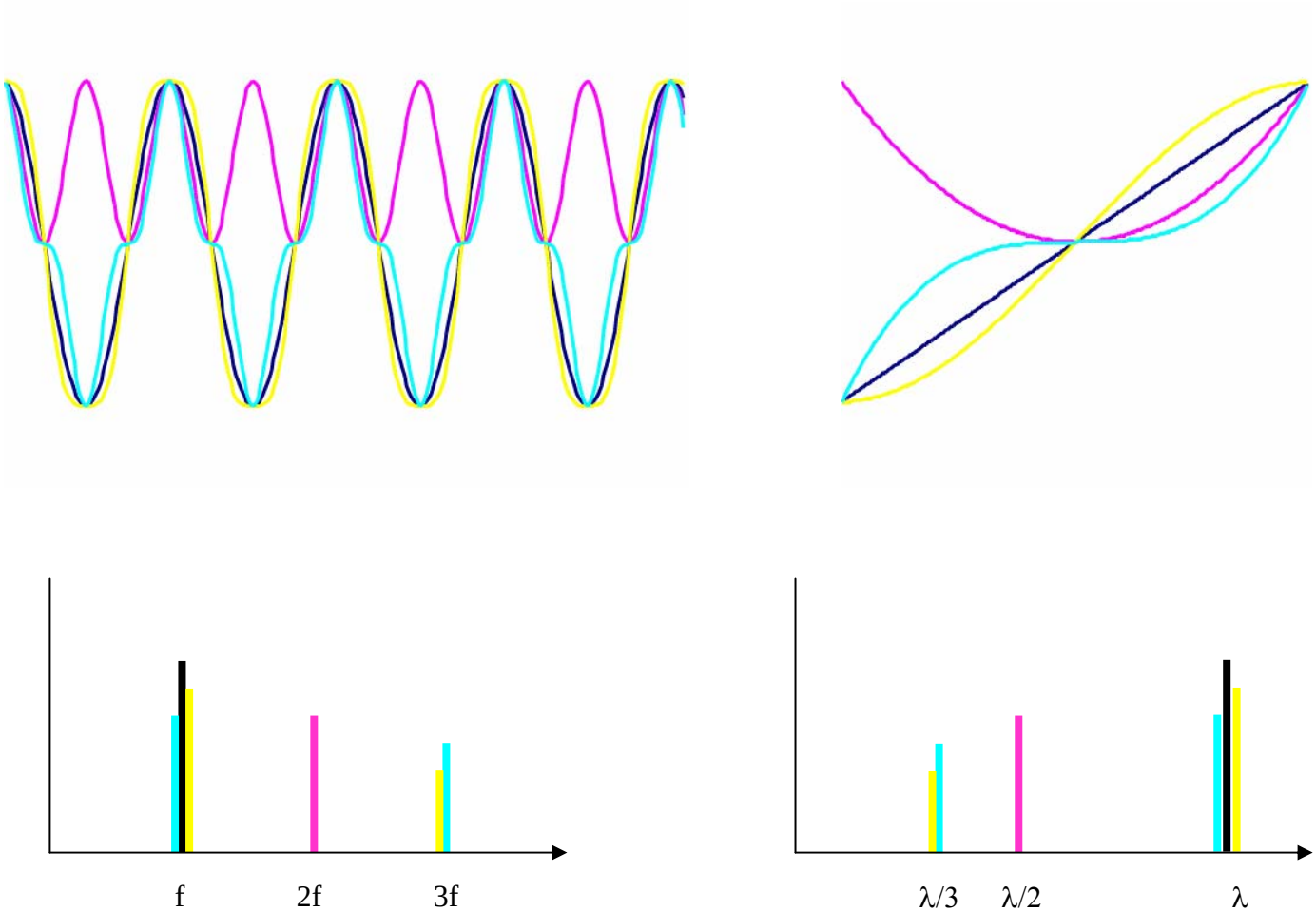
f
2f
3f
λ/3
λ/2
λ

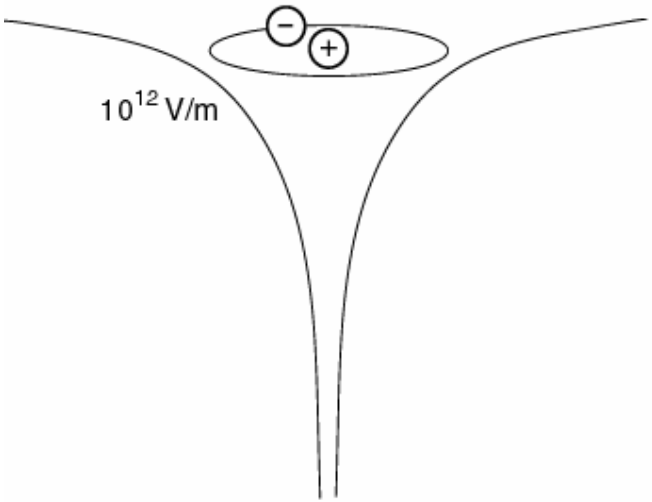

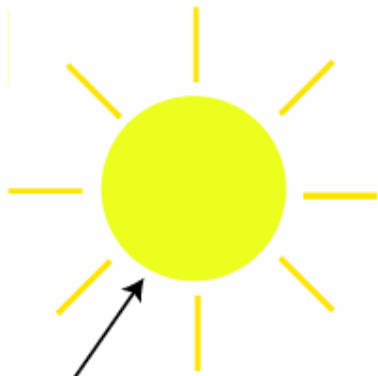

CW, 1mW : 10^{8} W/m^2 (10^{6} V/m)

100fs,100 MHz,10mW avg.: 10^{14} W/m^2 (10^{9} V/m)

100fs, 1mJ : 10^{22} W/m^2 (10^{13} V/m)

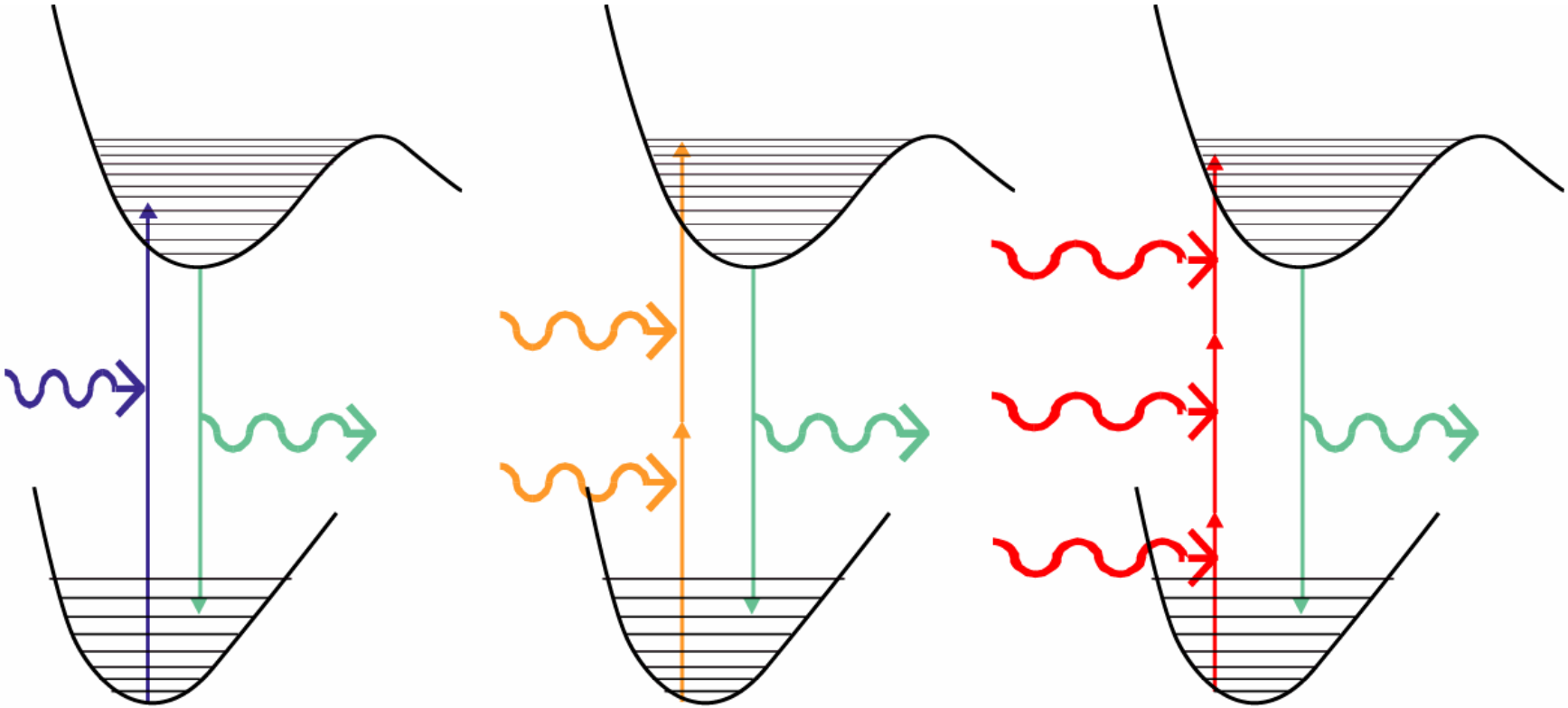

$$M + nP \rightarrow M^*$$

$$Rate \propto [P]^n$$

Rhodamine:

in the sun (100 mW/cm^2)

1P: 1/second

2P: 1/(10^7 years)

3P: <1/(age of the universe)

in pulsed laser focus (1 GW/cm^2 peak)

(1 mW average, 100 fs, 100 MHz)

1P: 1/ns

2P: 1/(10 ns)

3P: 1/ ms

Über Elementarakte mit zwei Quantensprüngen

Von Maria Göppert-Mayer

(Göttinger Dissertation)

(Mit 5 Figuren)

Einleitung

Der erste Teil dieser Arbeit beschäftigt sich mit dem Zusammenwirken zweier Lichtquanten in einem Elementarakt. Mit Hilfe der Diracschen Dispersionstheorie[1]) wird die Wahrscheinlichkeit eines dem Ramaneffekt analogen Prozesses, nämlich der Simultanemission zweier Lichtquanten, berechnet. Es zeigt sich, daß eine Wahrscheinlichkeit dafür besteht, daß ein angeregtes Atom seine Anregungsenergie in zwei Lichtquanten aufteilt, deren Energien in Summe die Anregungsenergie ergeben, aber sonst beliebig sind. Fällt auf das Atom Licht, dessen Frequenz kleiner ist, als die entsprechende Eigenfrequenz des Atoms, so tritt außerdem noch eine erzwungene Doppelemission hinzu, bei der das Atom seine Energie in ein Lichtquant der eingesandten und eins der Differenzfrequenz aufteilt. Kramers und Heisenberg[2]) haben die Wahrscheinlichkeit dieses letzteren Prozesses korrespondenzmäßig berechnet.

Außerdem wird die Umkehrung dieses Prozesses betrachtet, nämlich der Fall, daß zwei Lichtquanten, deren Frequenzsumme gleich der Anregungsfrequenz des Atoms ist, zusammenwirken, um das Atom anzuregen.

Ferner wird untersucht, wie sich ein Atom gegenüber stoßenden Teilchen verhalten kann, wenn es gleichzeitig die Möglichkeit hat, spontan Licht zu emittieren. Oldenberg[3]) findet experimentell eine Verbreiterung der Resonanzlinie des Quecksilbers, wenn er die angeregten Atome vielfach mit lang-

1) P. A. M. Dirac, Proc. of R. S. vol. 114. S. 143 u. 710. 1927.
2) H. A. Kramers u. W. Heisenberg, Ztschr. f. Phys. 31. S. 681. 1925.
3) O. Oldenberg, Ztschr. f. Phys. 51. S. 605. 1928.

Annalen der Physik **9**: 273. (1931).

TWO-PHOTON EXCITATION IN $CaF_2:Eu^{2+}$

W. Kaiser and C. G. B. Garrett
Bell Telephone Laboratories, Murray Hill, New Jersey
(Received August 28, 1961)

With the development of optical masers,[1-3] it is now possible to study two-photon processes which necessitate intense sources of monochromatic radiation. We have investigated the generation of blue fluorescent light around $\lambda_b = 4250$ A by illuminating $CaF_2:Eu^{2+}$ crystals with red light, $\lambda_r = 6943$ A, of a ruby optical maser.[2] Our experiments differ from the recent investigations by Franken et al.,[4] who observed the generation of optical harmonics in quartz. It is essential in their experiments that the crystal lacks a center of inversion and that it is transparent at ν_r and $2\nu_r$. In our investigations, the highly symmetric cubic CaF_2 structure is used and after an excitation to a real absorbing state of Eu^{2+} at $2\nu_r$, the fluorescent decay to a lower state is observed. CaF_2 crystals, with 0.1% Eu^{2+} ions substituted for Ca^{2+}, exhibit strong absorption between 30 000 and 25 000 cm^{-1} resulting from electronic $4f \rightarrow 5d$ transitions of the Eu^{2+} ion.[5] Excitation of $CaF_2:Eu^{2+}$ with light absorbed in this wavelength range gives rise to a brilliant blue fluorescence (bandwidth ~300 A) which originates at levels responding to the diameter of the incident light beam. When pure CaF_2 was illuminated by the optical maser in the same way, no light with $\lambda < \lambda_r$ was observed on the photographic plate. This observation is expected from the high symmetry of the CaF_2 lattice.

In a second experiment, the light beam leaving the quartz spectrometer was intersected by two mirrors in such a way that the red and blue parts of the spectrum were directed separately onto two photomultipliers. The signals of these photomultipliers were displayed simultaneously on a dual-beam oscilloscope. Load resistors of 10^5 ohms in the photomultiplier circuit were employed in order to smooth out the spikes (resulting from the relaxation oscillations) of the ruby optical maser and to allow a direct quantitative comparison between the two signals. In Fig. 2 the signal I_b obtained in the blue part of the spectrum is plotted against the signal in the red I_r, which is a direct measure of intensity incident on the crystal. The empirical line through our experimental points represents the quadratic relation $I_b \propto I_r^2$,

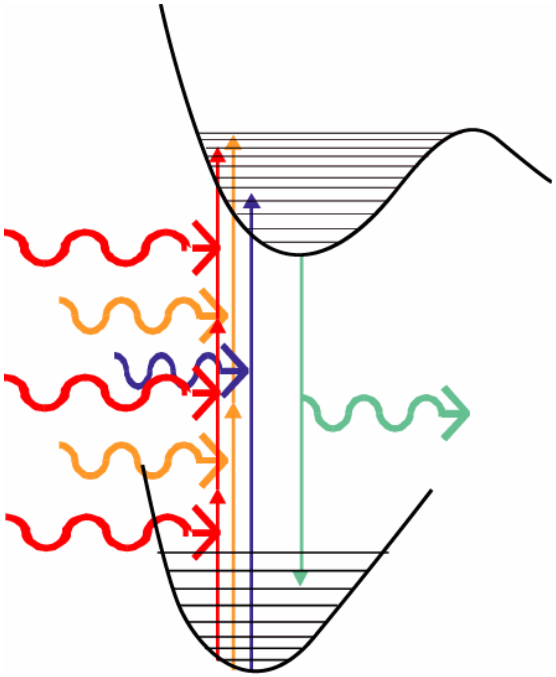

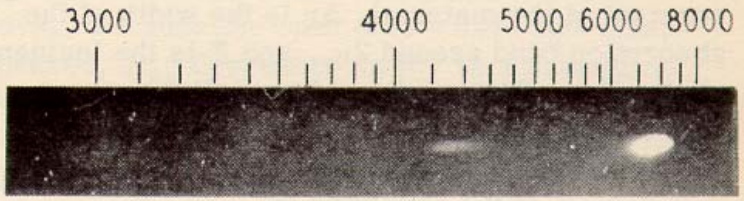

FIG. 1. Positive of photographic plate, indicating the blue emission of a $CaF_2:Eu^{2+}$ crystal under strong illumination with $\lambda_\gamma = 6943$ A.

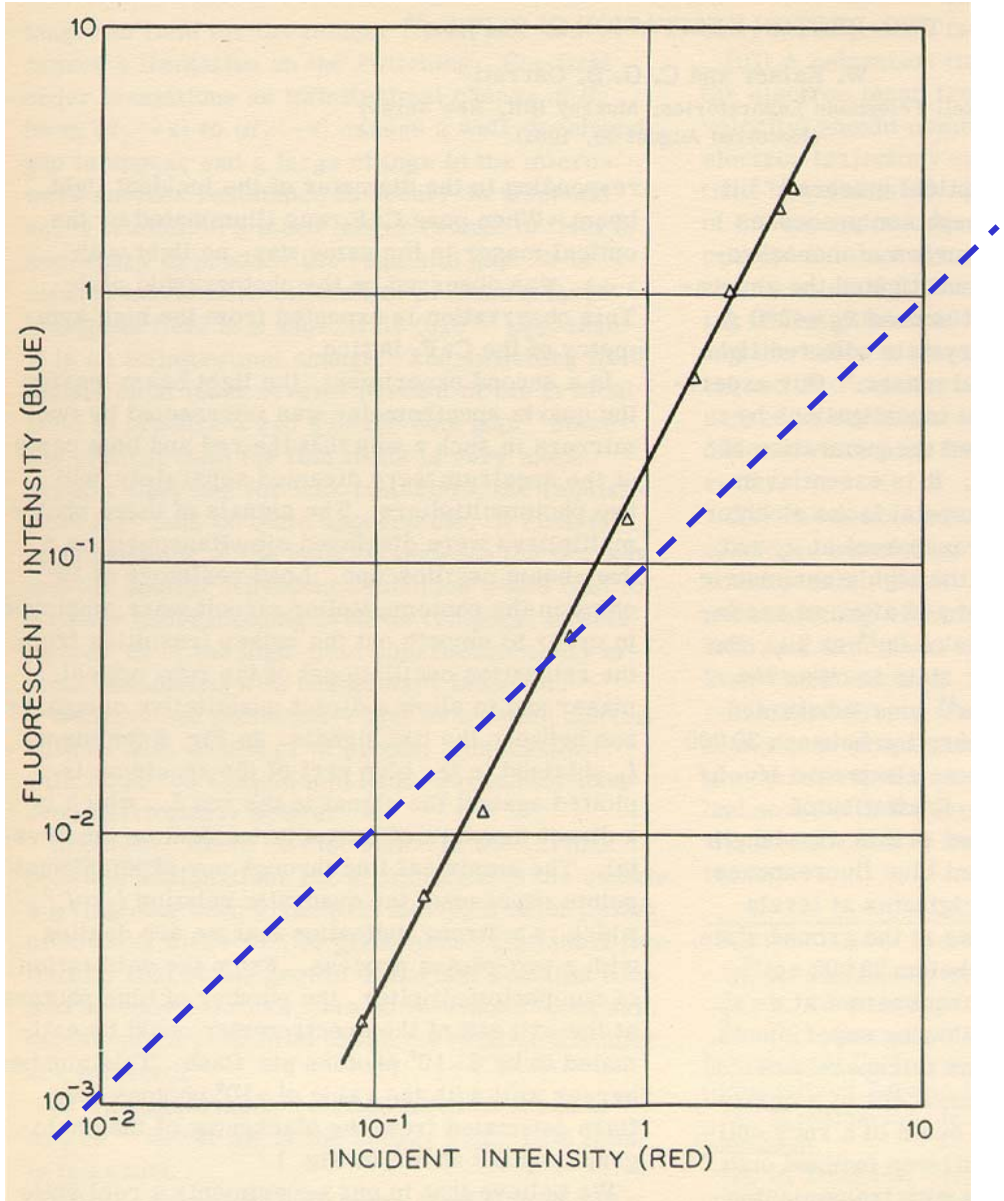

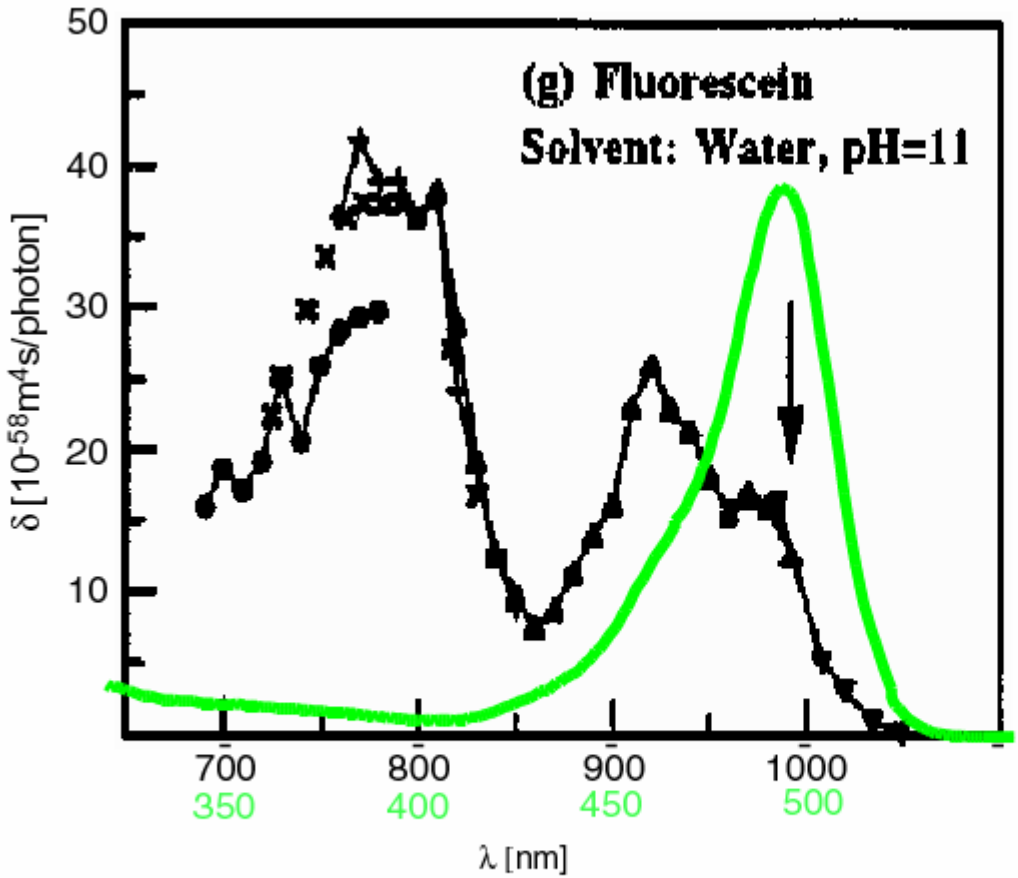

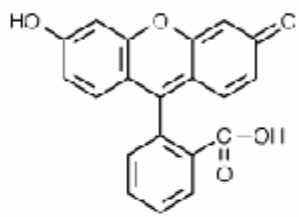

from: Xu, C. and W. W. Webb, JOSA-B **13**: 481-491 (1996)

$$W_{i\to f} = 128\pi^3\alpha^2 I^2\omega^2 g_f \left| \sum_n \frac{\left\langle f \left| \vec{\mathbf{e}} \bullet \vec{\mathbf{r}} \right| n \right\rangle \left\langle n \left| \vec{\mathbf{e}} \bullet \vec{\mathbf{r}} \right| i \right\rangle}{\omega_{ni} - \omega} \right|^2$$

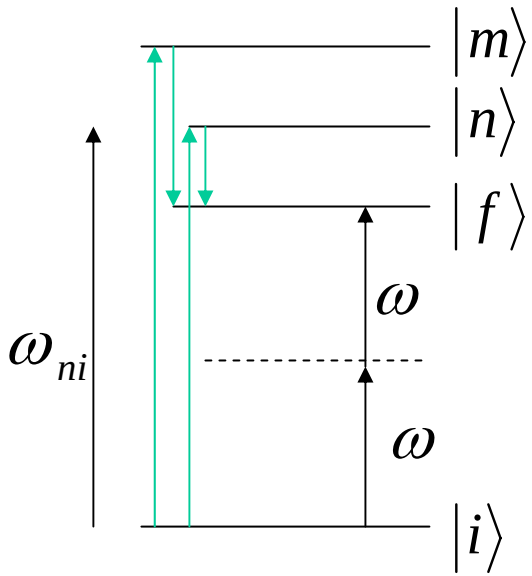

α	finestructure constant,
I	photon flux density,
g_f	density of states,
$\vec{\mathbf{e}}$	polarization vector
$\vec{r}$	position operator

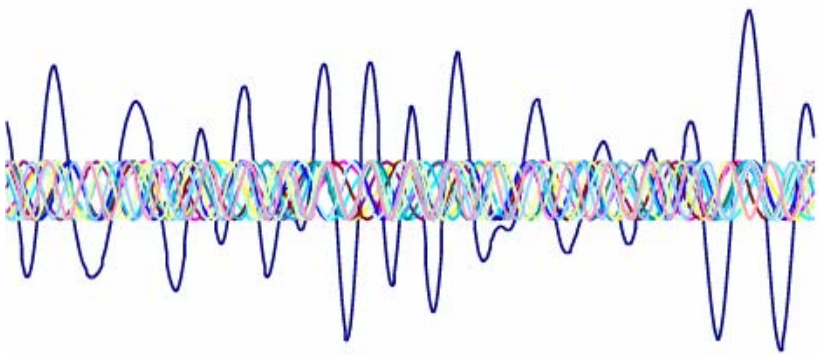

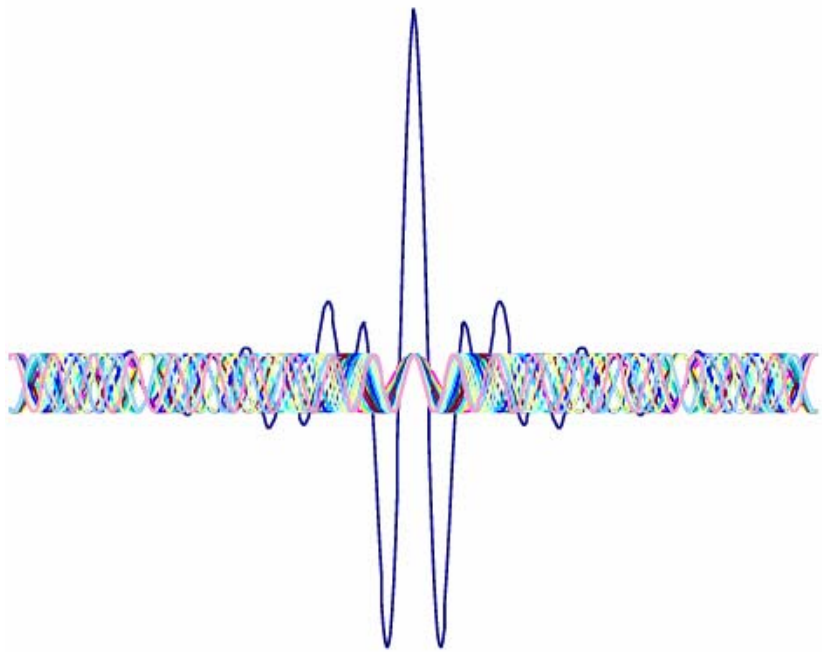

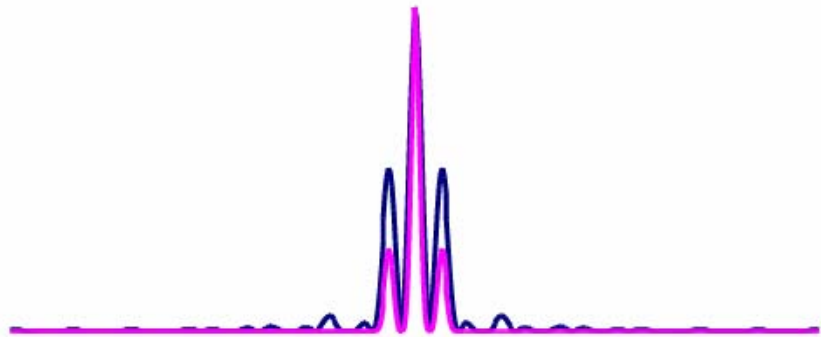

http://en.wikipedia.org/wiki/Kerr-lens_modelocking

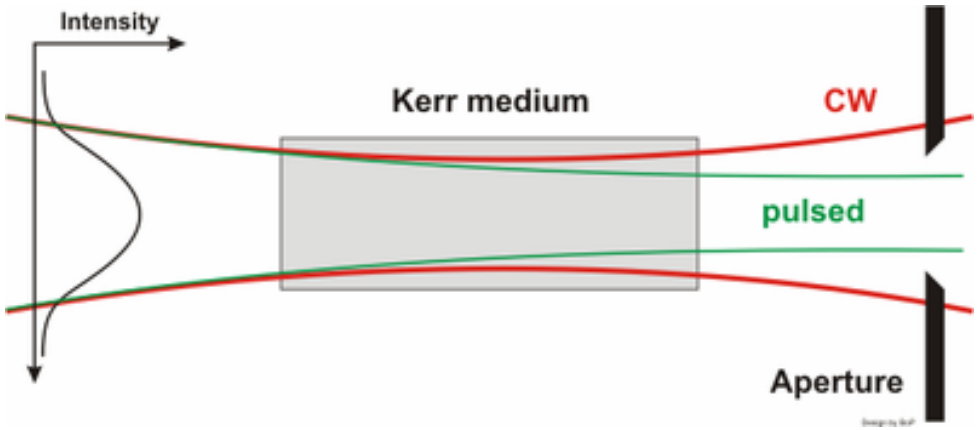

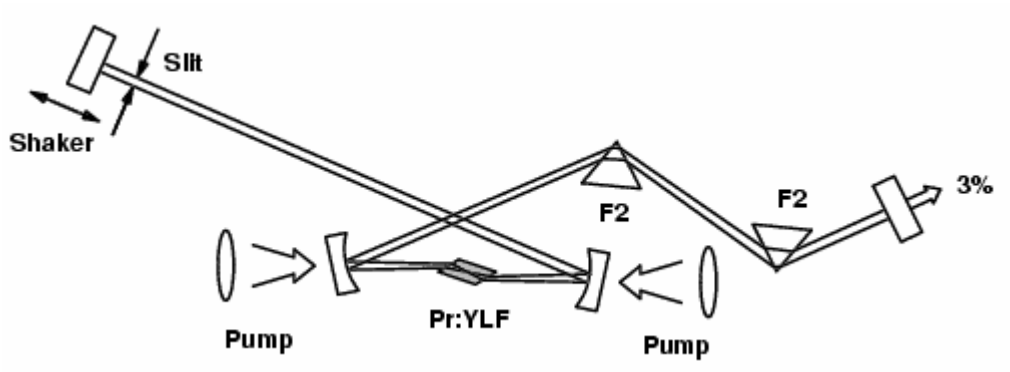

http://www.imperial.ac.uk/research/photonics/research/topics/lasers/images/pr-cavity.gif

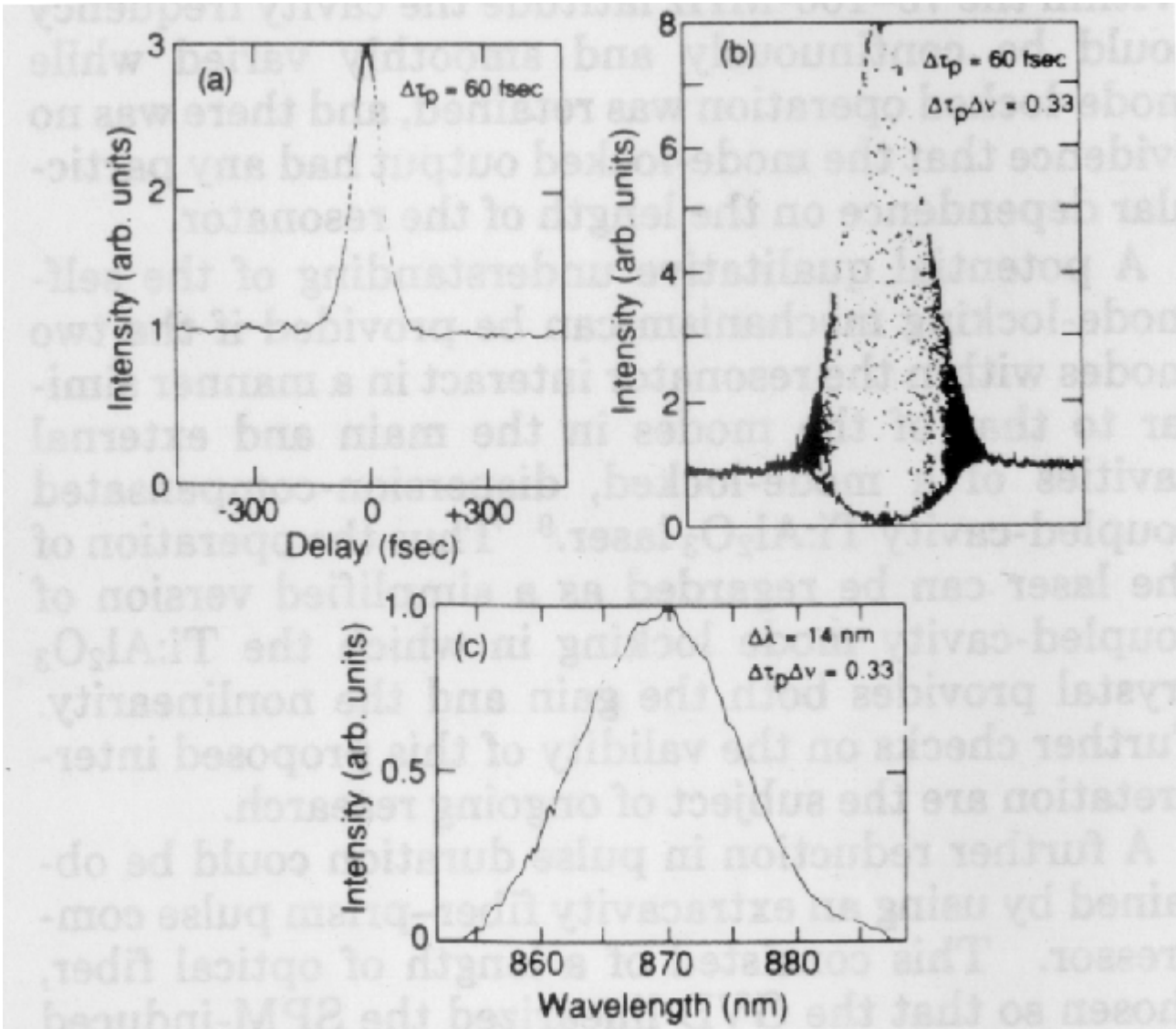

Fig. 3. (a) Intensity and (b) interferometric autocorrelation traces and (c) the associated spectrum for the mode-locked Ti:Al_2O_3 laser.

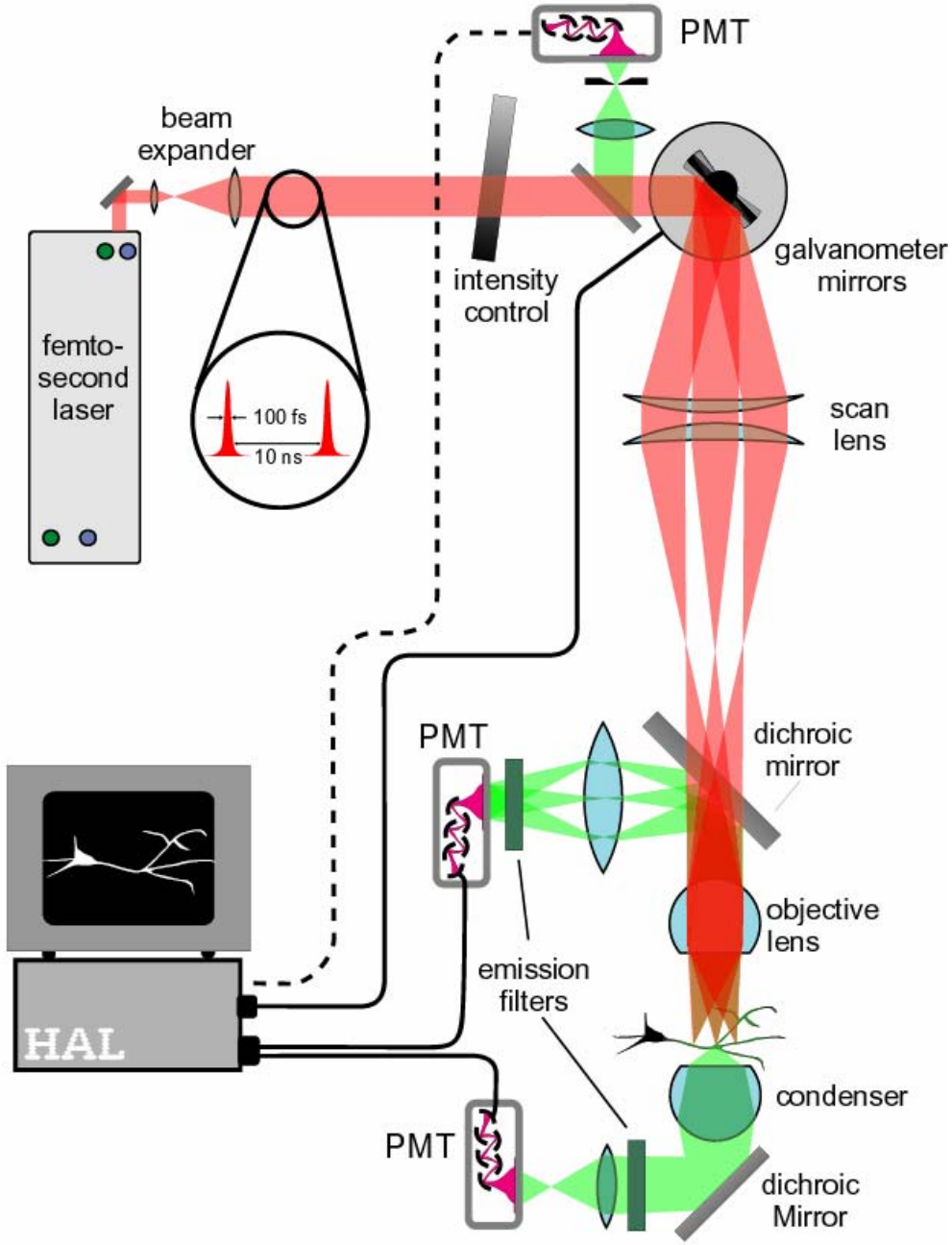
PMT
beam
expander
intensity
control
galvanometer
mirrors
femto-
second
laser
100 fs
10 ns
scan
lens
PMT
dichroic
mirror
objective
lens
emission
filters
HAL
condenser
PMT
dichroic
Mirror

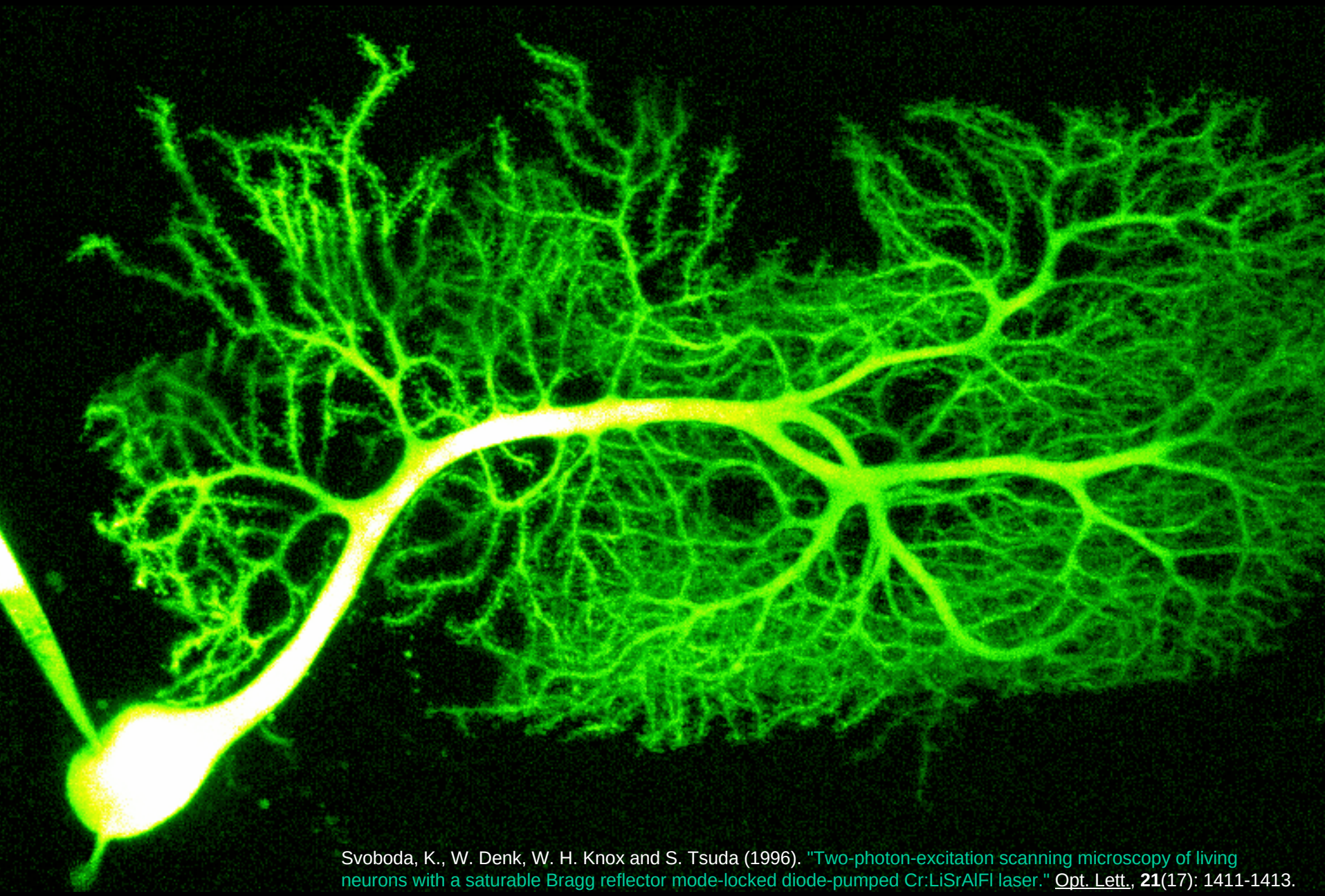

Svoboda, K., W. Denk, W. H. Knox and S. Tsuda (1996). "Two-photon-excitation scanning microscopy of living neurons with a saturable Bragg reflector mode-locked diode-pumped Cr:LiSrAlFl laser." Opt. Lett., **21**(17): 1411-1413.

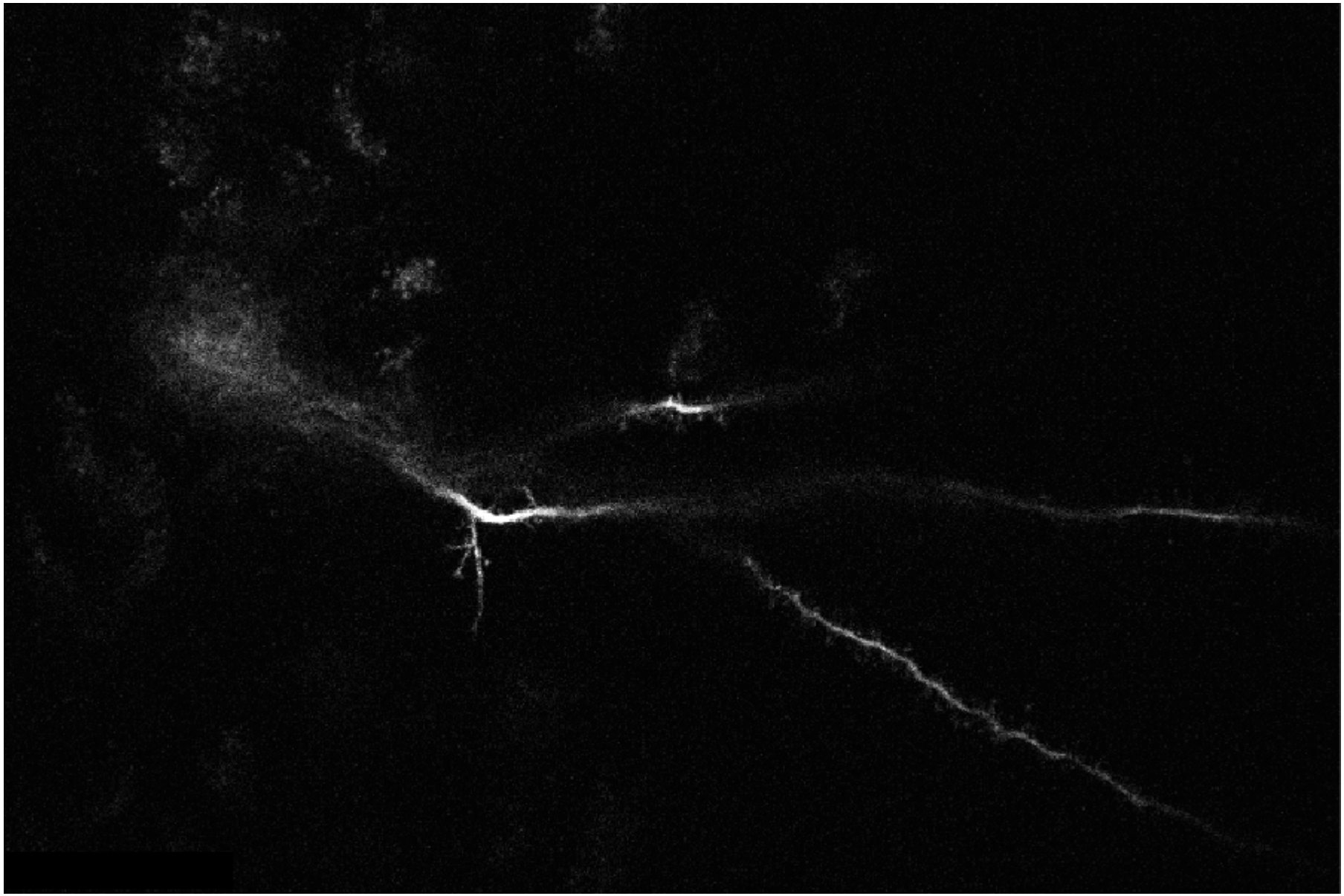

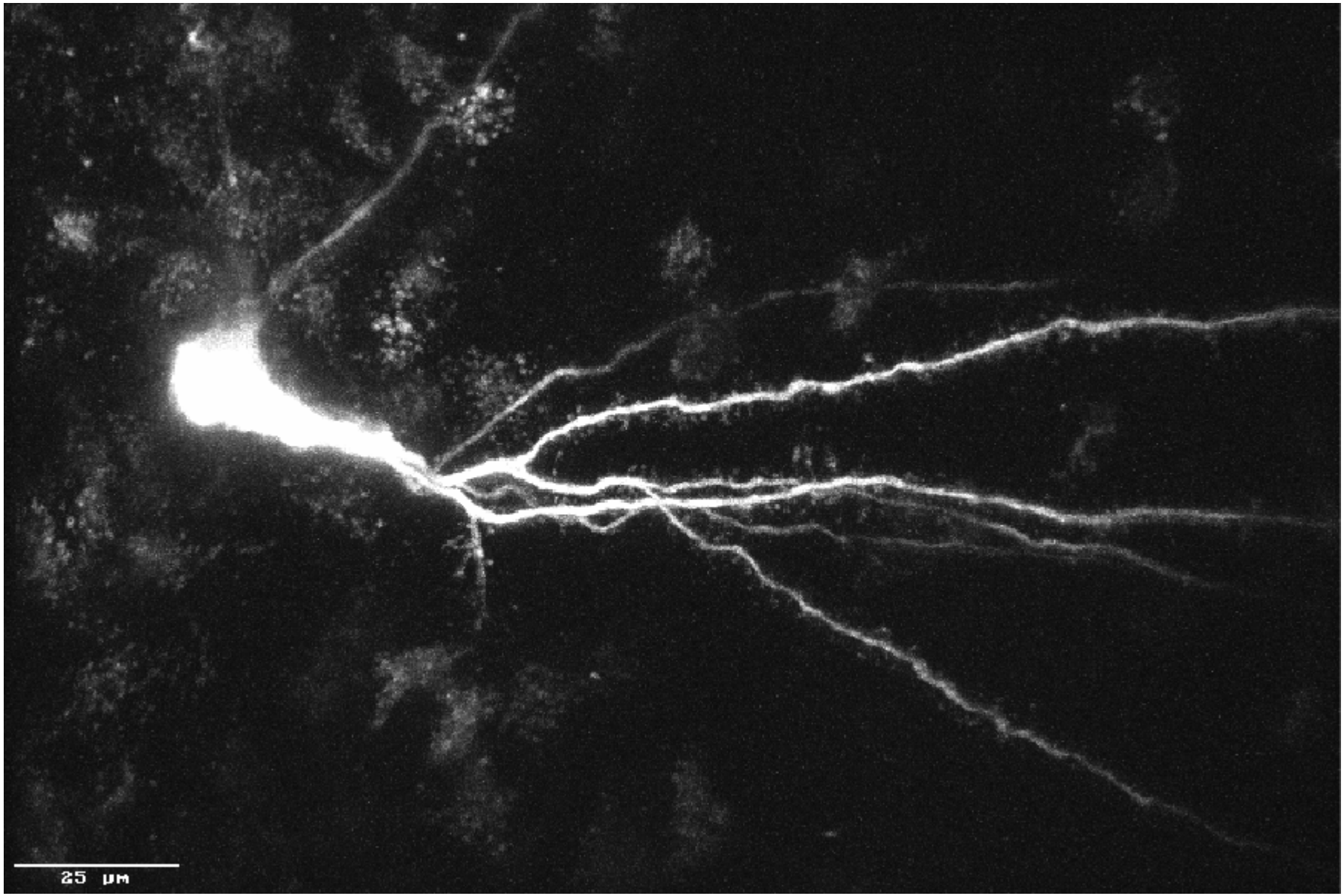
25 µm

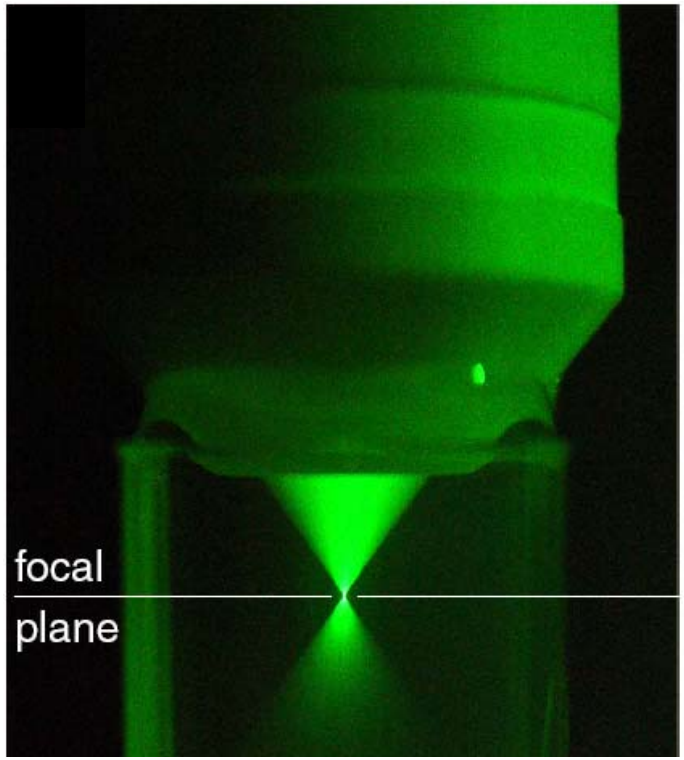

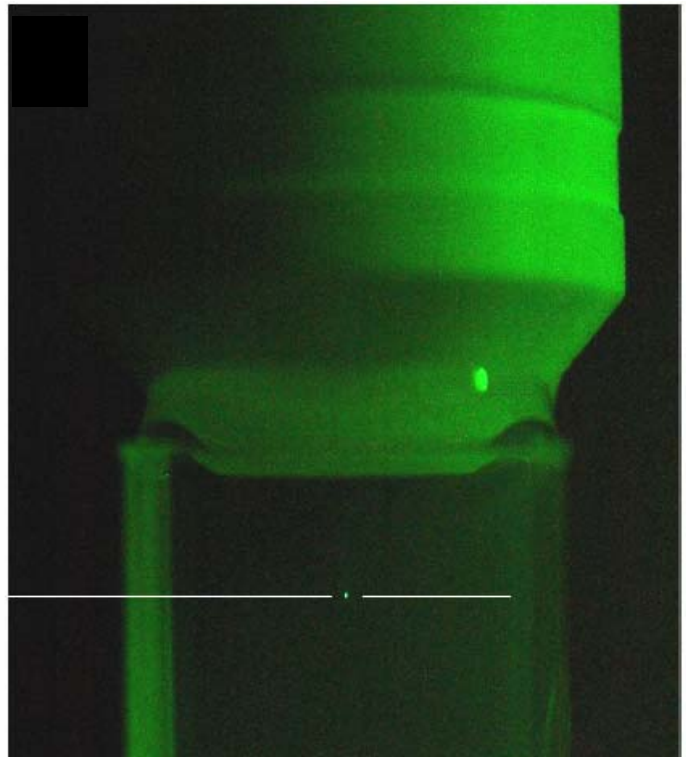

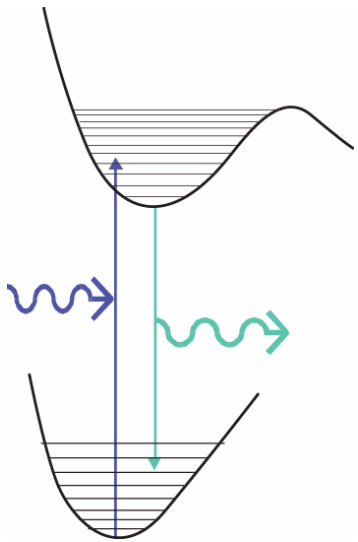

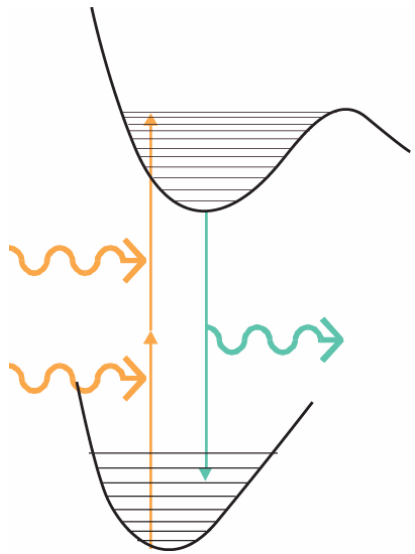

Patrick Theer…

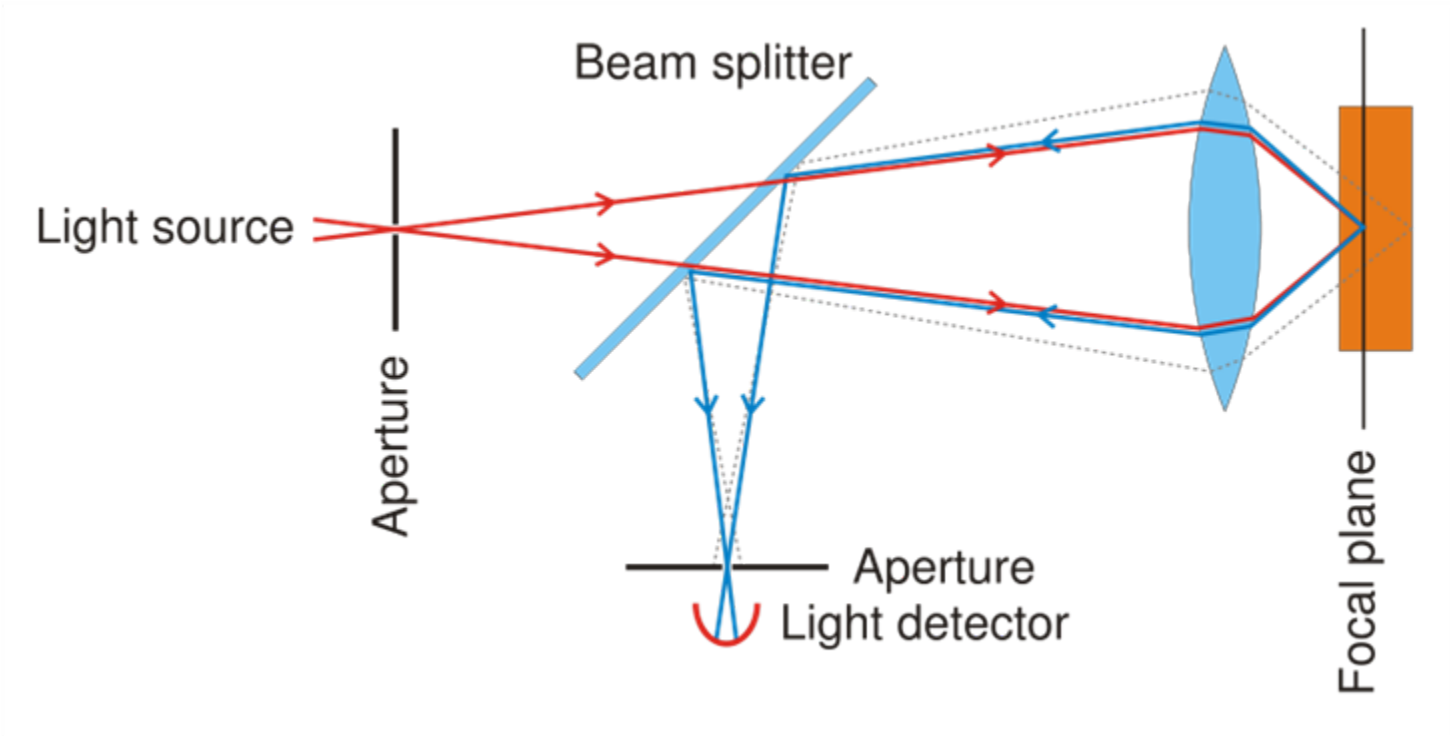

http://upload.wikimedia.org/wikipedia/en/thumb/9/9f/Confocalprinciple.svg/800px-Confocalprinciple.svg.png

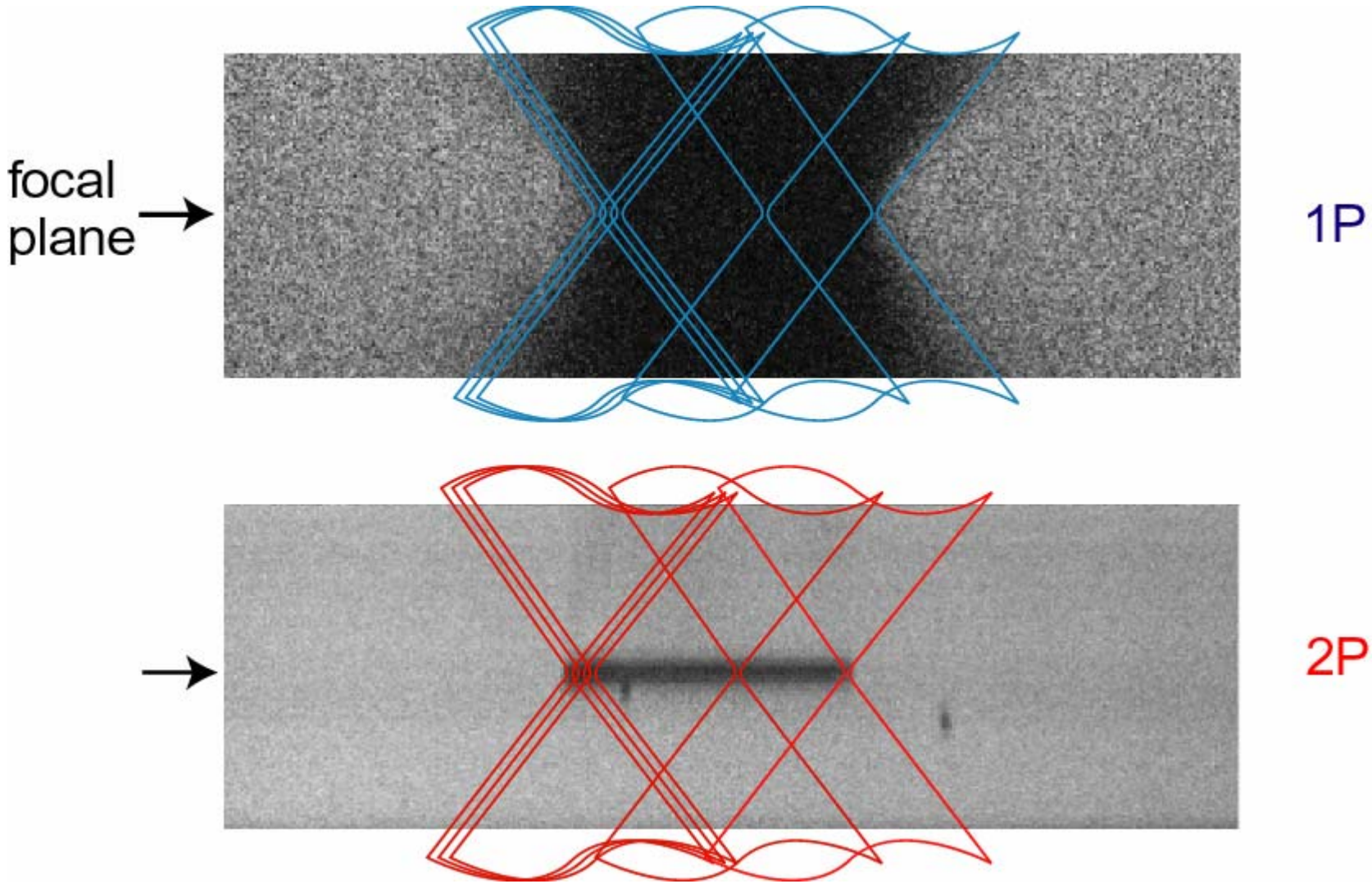
focal
plane
1P
2P

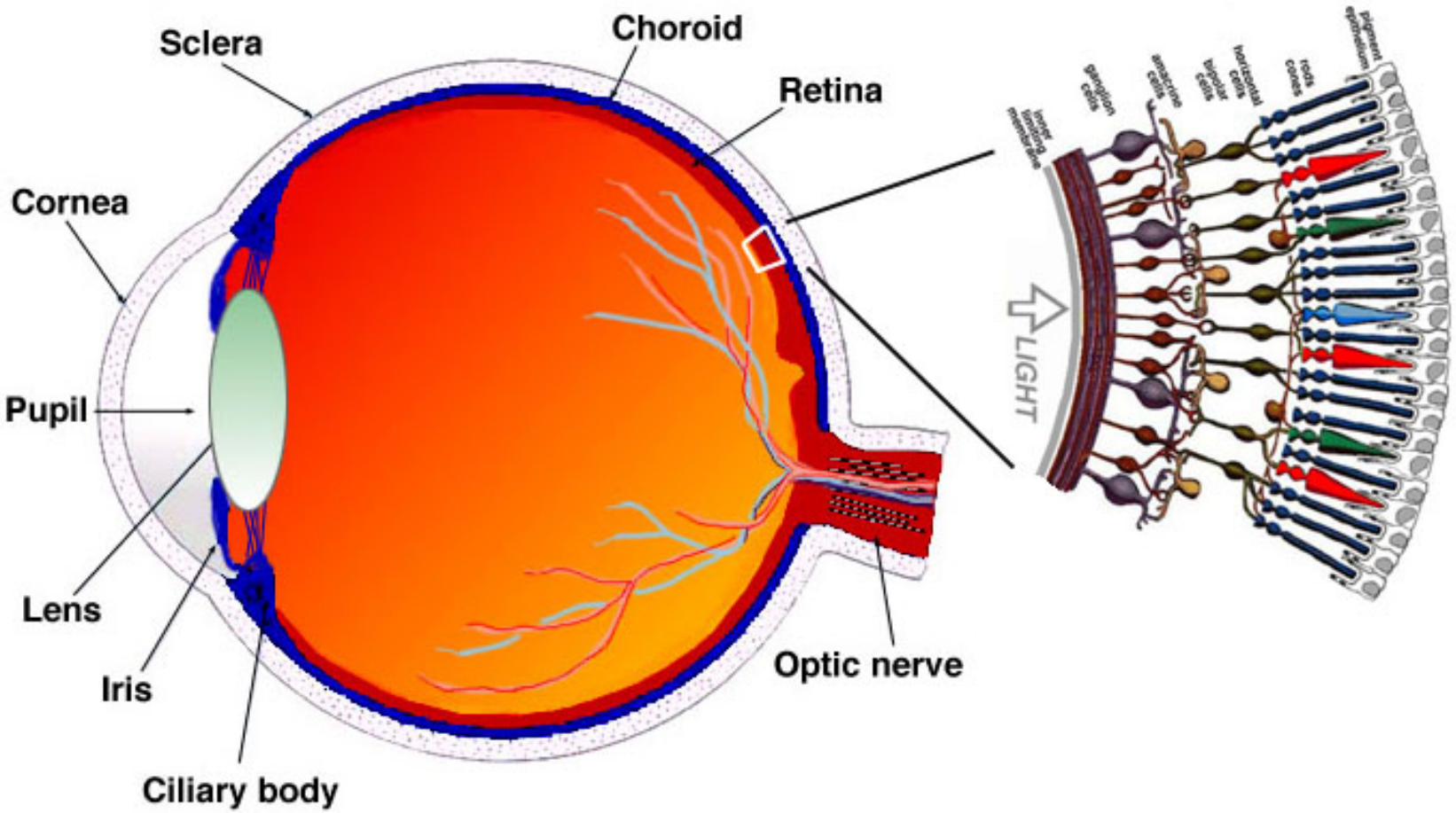
Sclera
Choroid
Retina
Cornea
Pupil
Lens
Iris
Ciliary body
Optic nerve
LIGHT

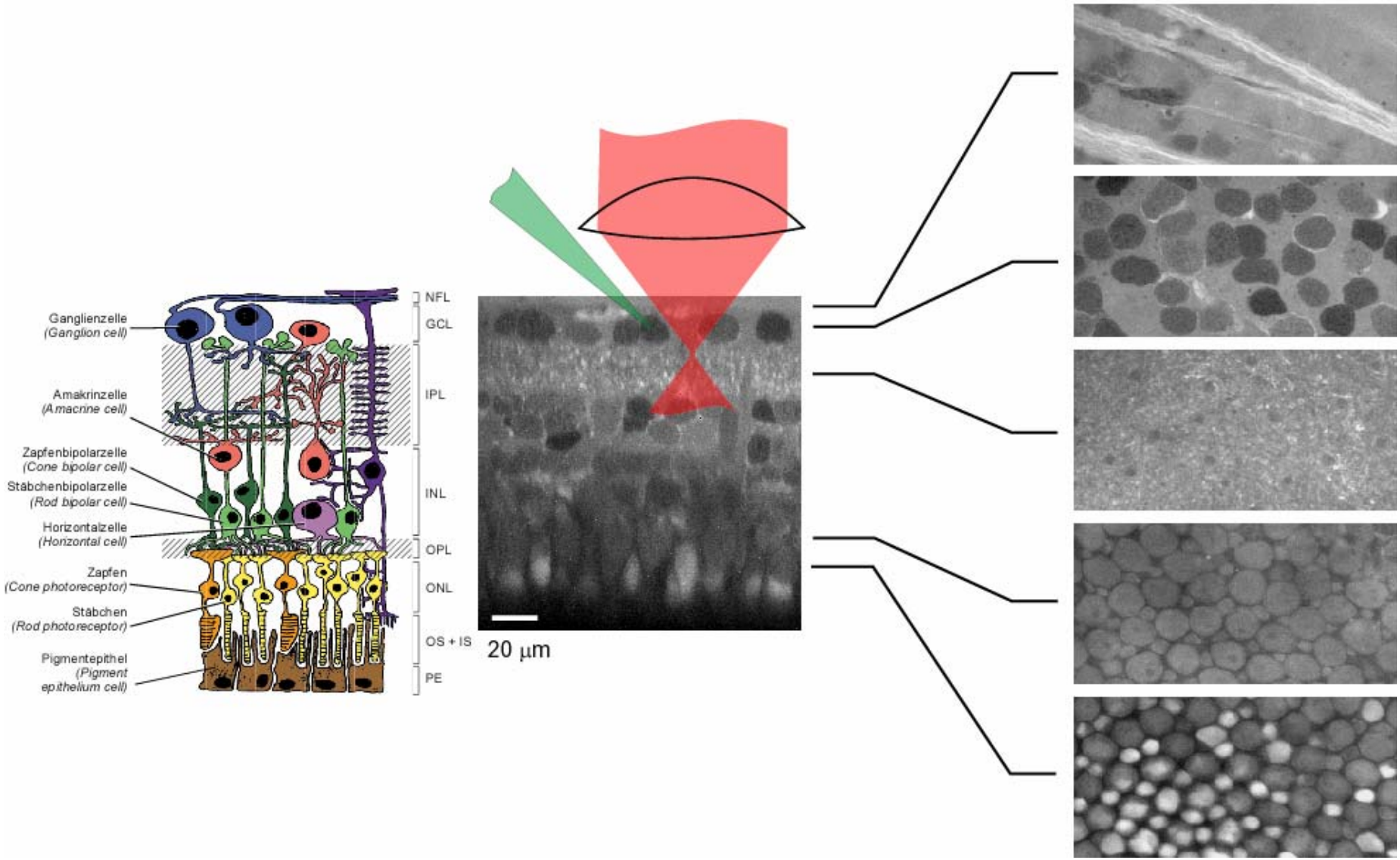
Ganglienzelle
(Ganglion cell)
Amakrinzelle
(Amacrine cell)
Zapfenbipolarzelle
(Cone bipolar cell)
Stäbchenbipolarzelle
(Rod bipolar cell)
Horizontalzelle
(Horizontal cell)
Zapfen
(Cone photoreceptor)
Stäbchen
(Rod photoreceptor)
Pigmentepithel
(Pigment
epithelium cell)
NFL
GCL
IPL
INL
OPL
ONL
OS + IS
PE
20 µm

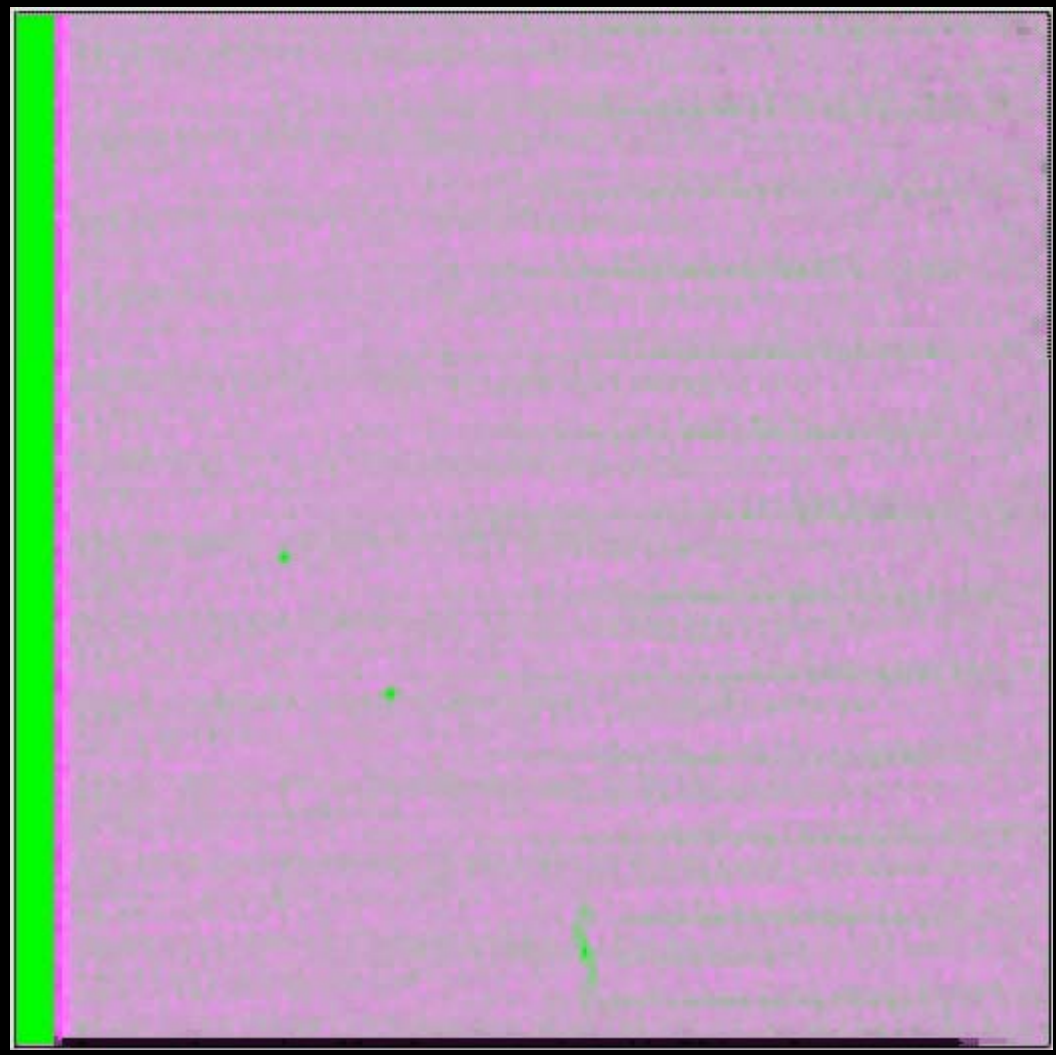

Thomas Euler….

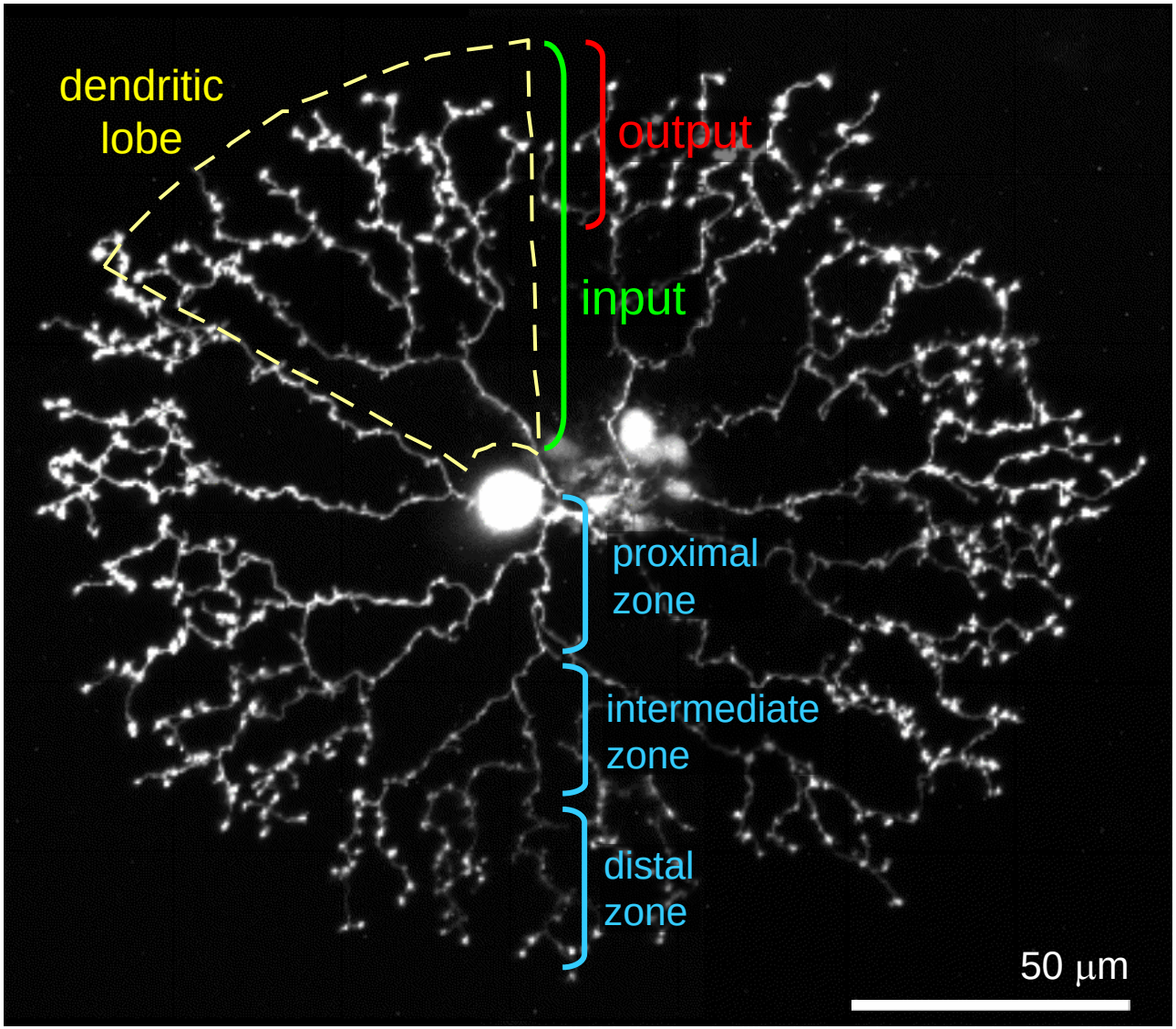

Thomas Euler….

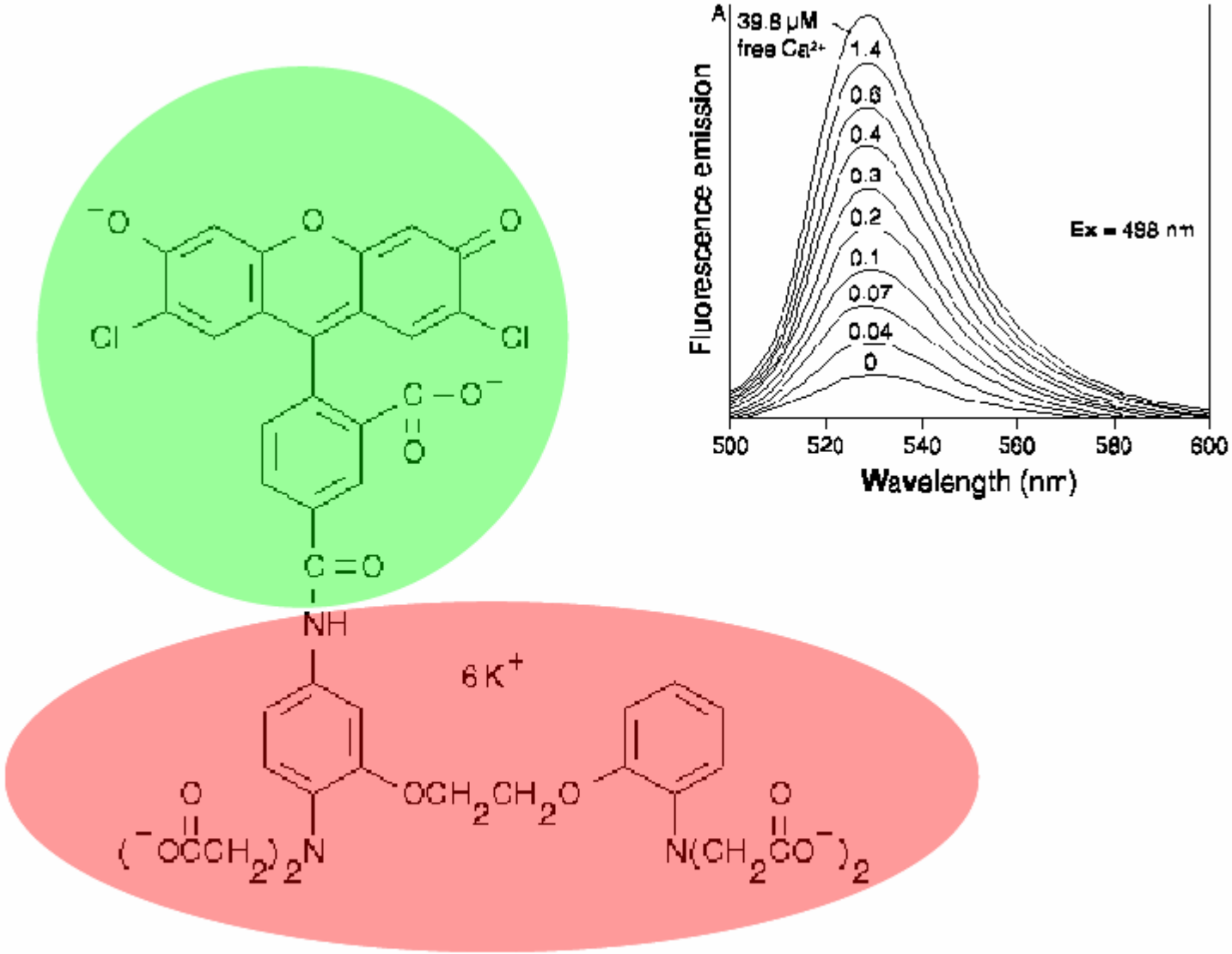

Handbook of Fluorescent Probes and Research Chemicals by Richard Haugland

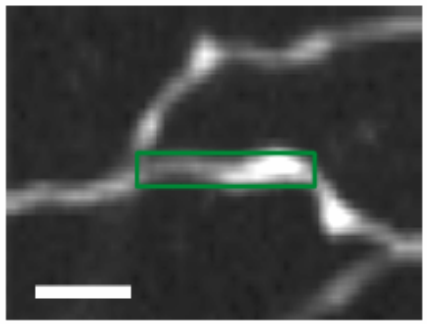

5μm

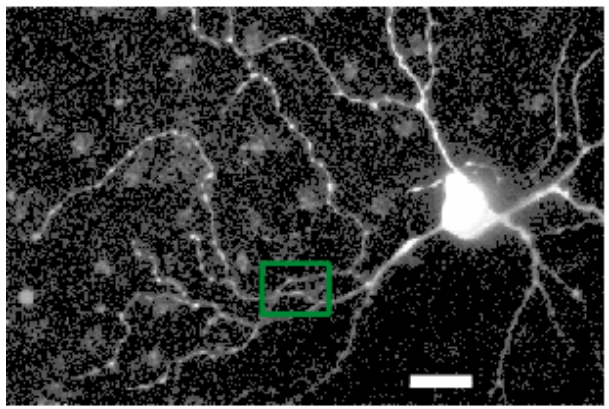

20μm

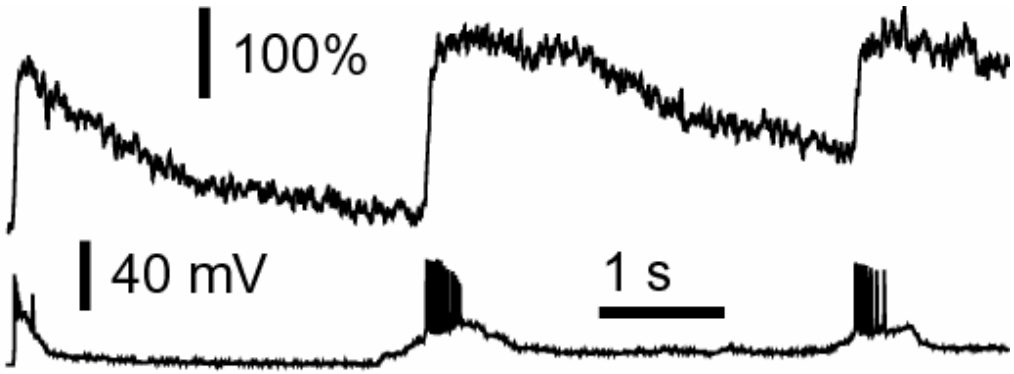

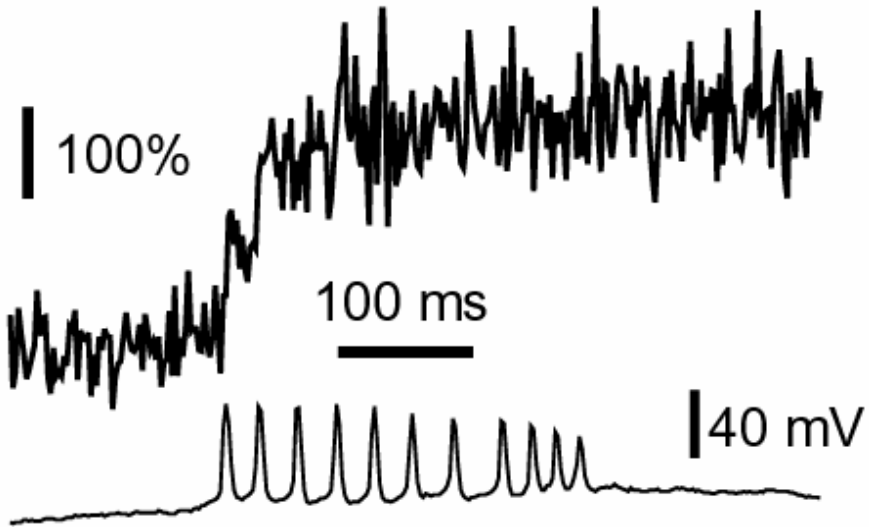

Two-photon OBIC: Experimental Setup

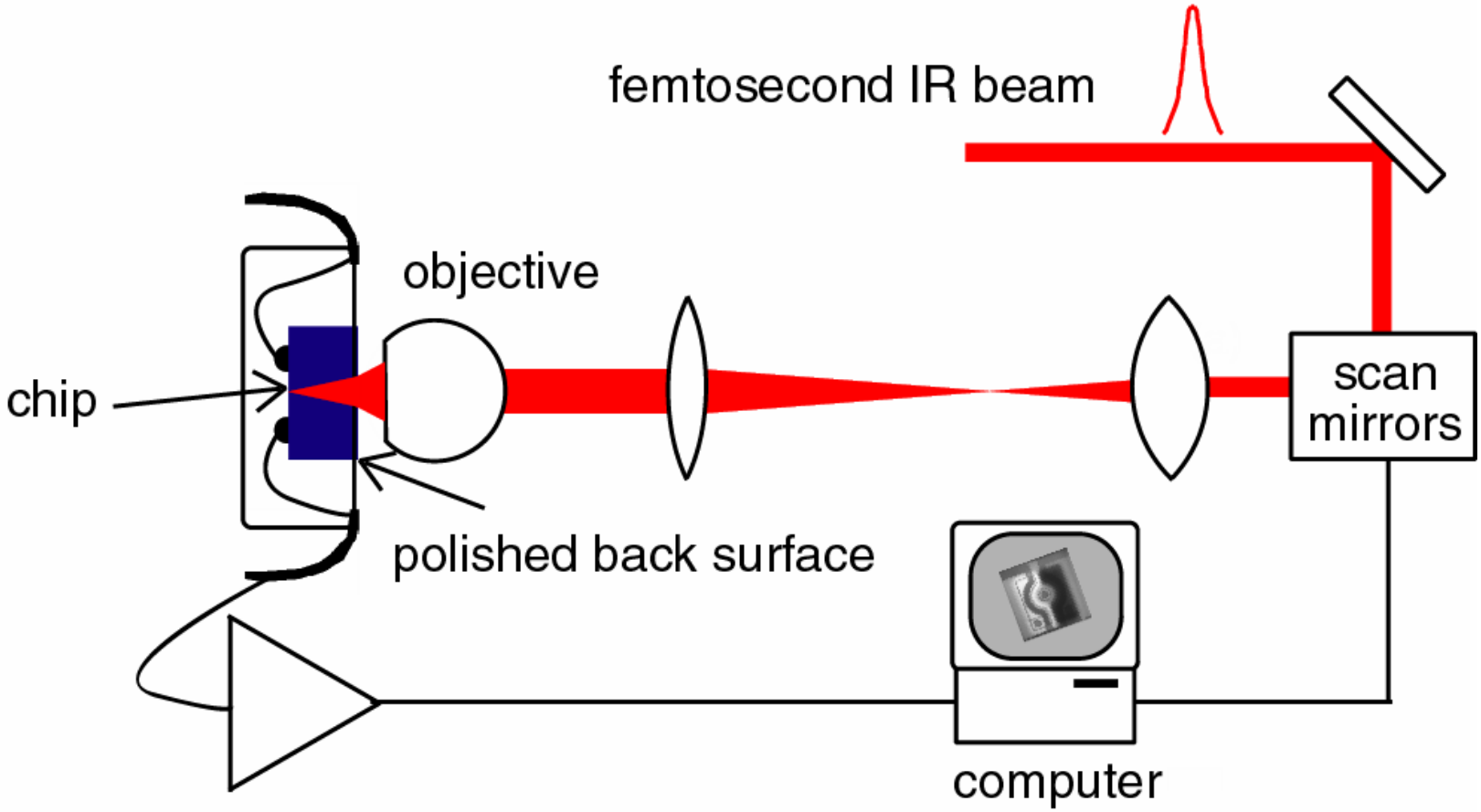

Xu, C. and W. Denk (1997).
"Two-photon optical beam induced current imaging through the backside of integrated circuits." Applied Physics Letters **71**(18): 2578-2580.

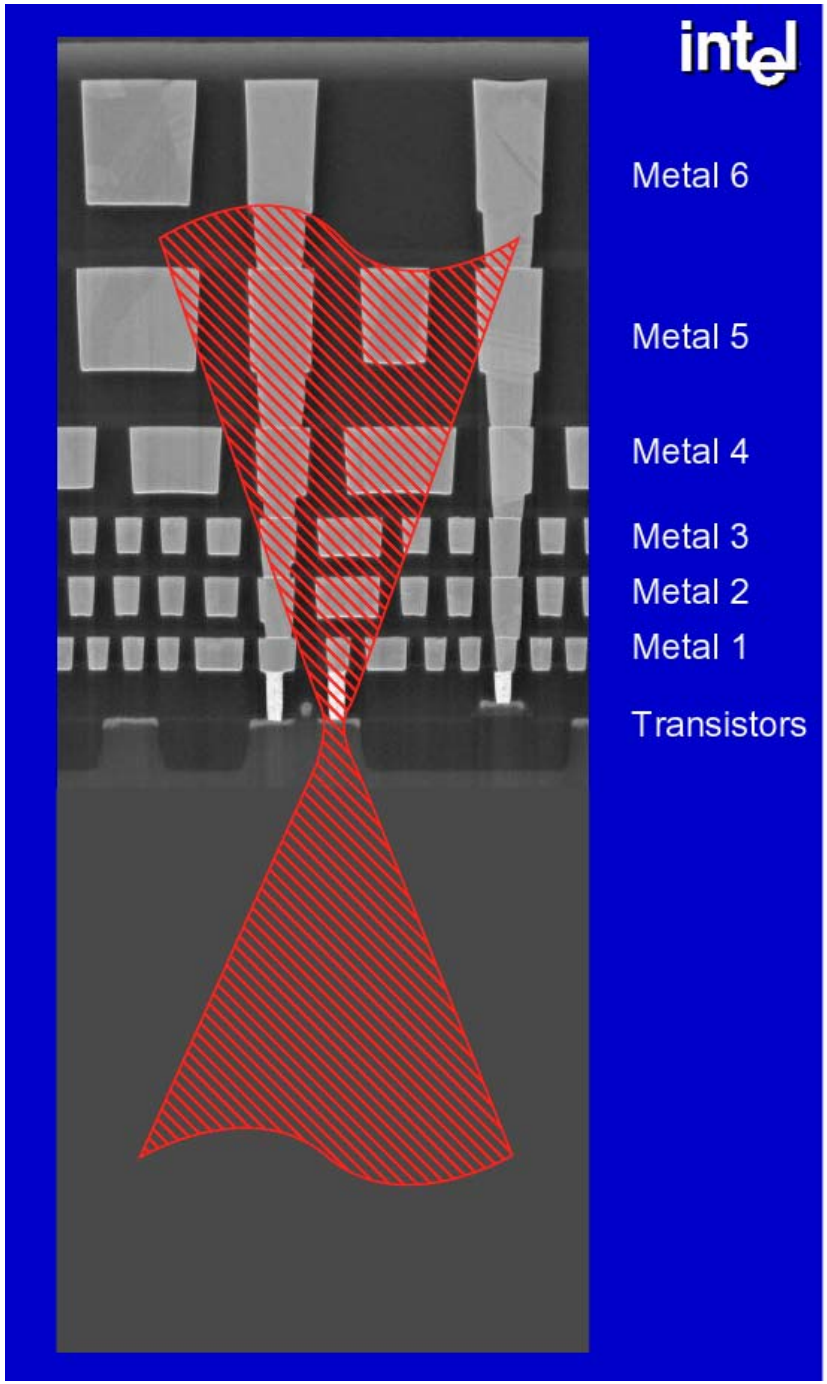
intel
Metal 6
Metal 5
Metal 4
Metal 3
Metal 2
Metal 1
Transistors

256X4K SRAM

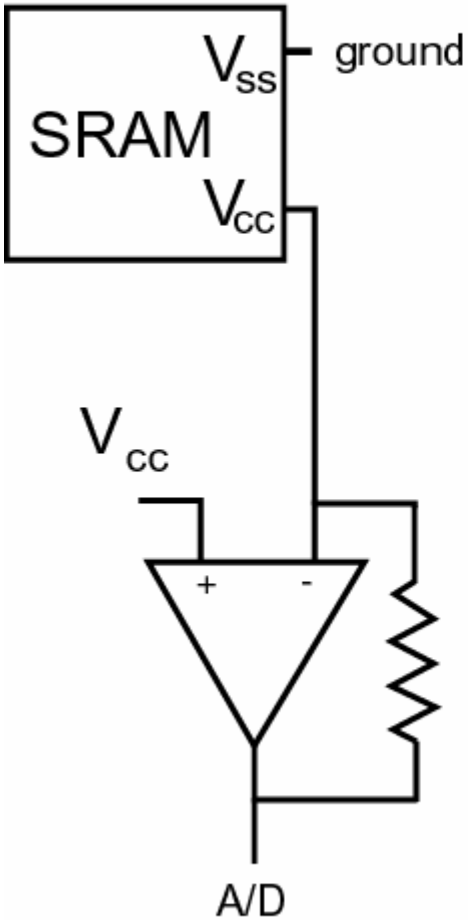

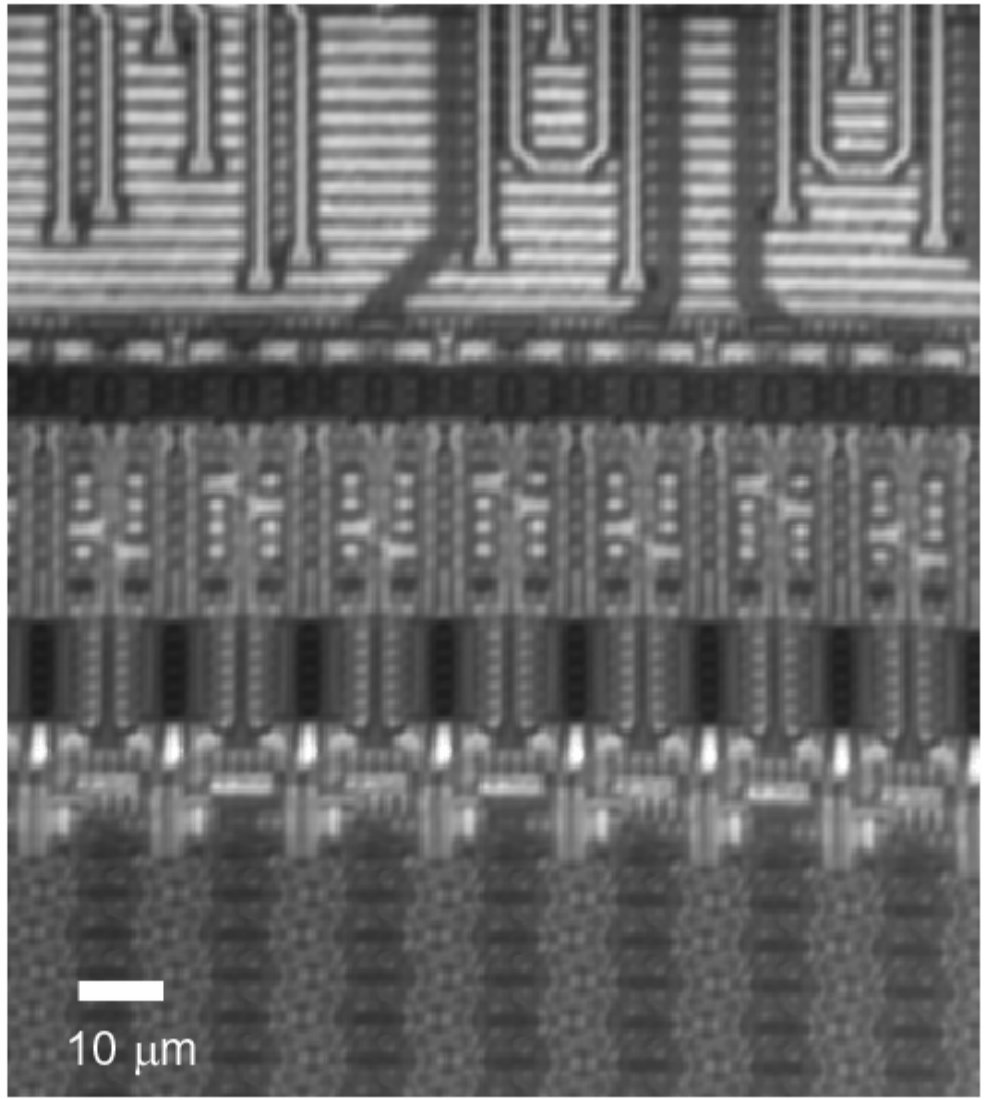

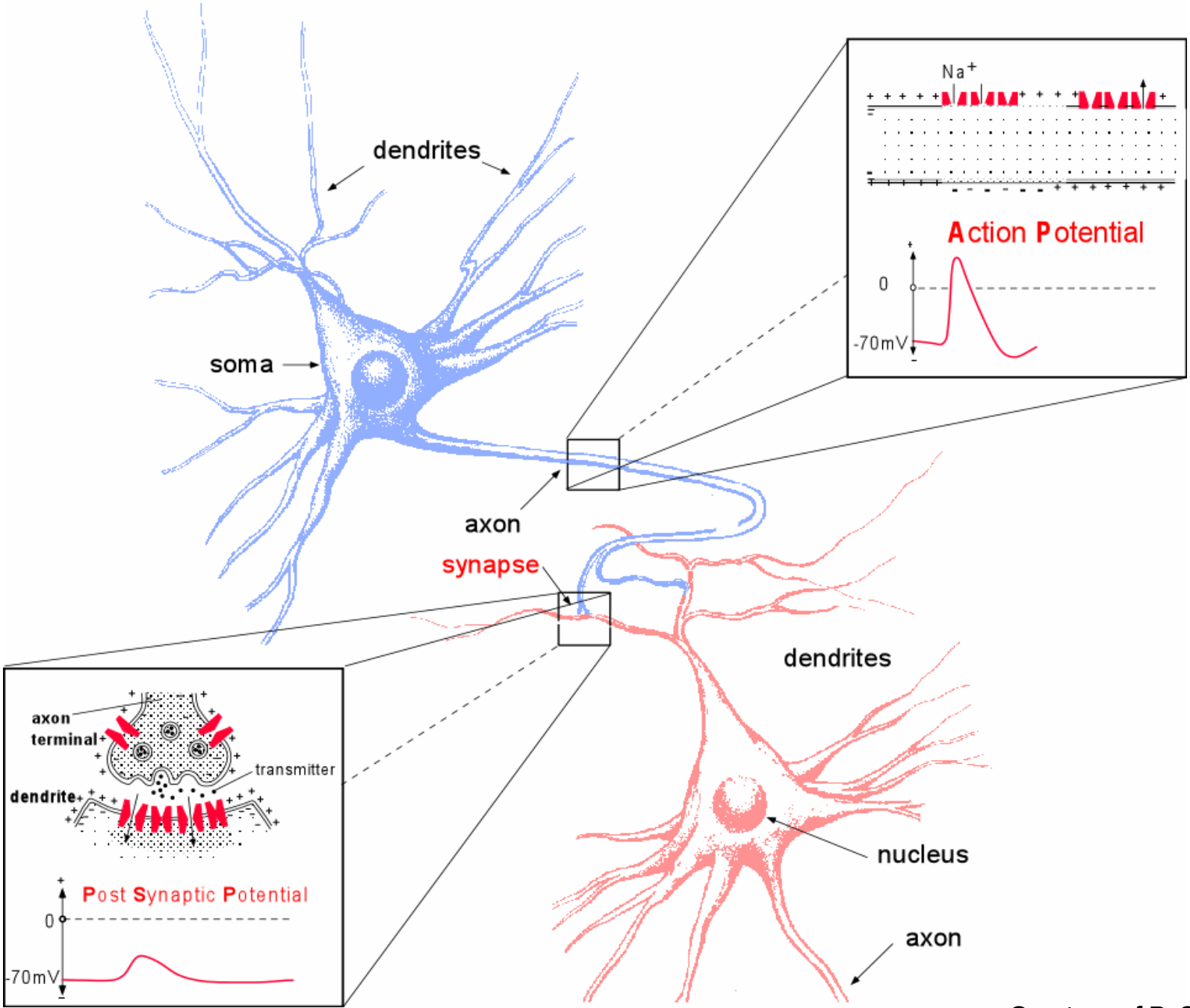

Courtesy of B. Sakmann

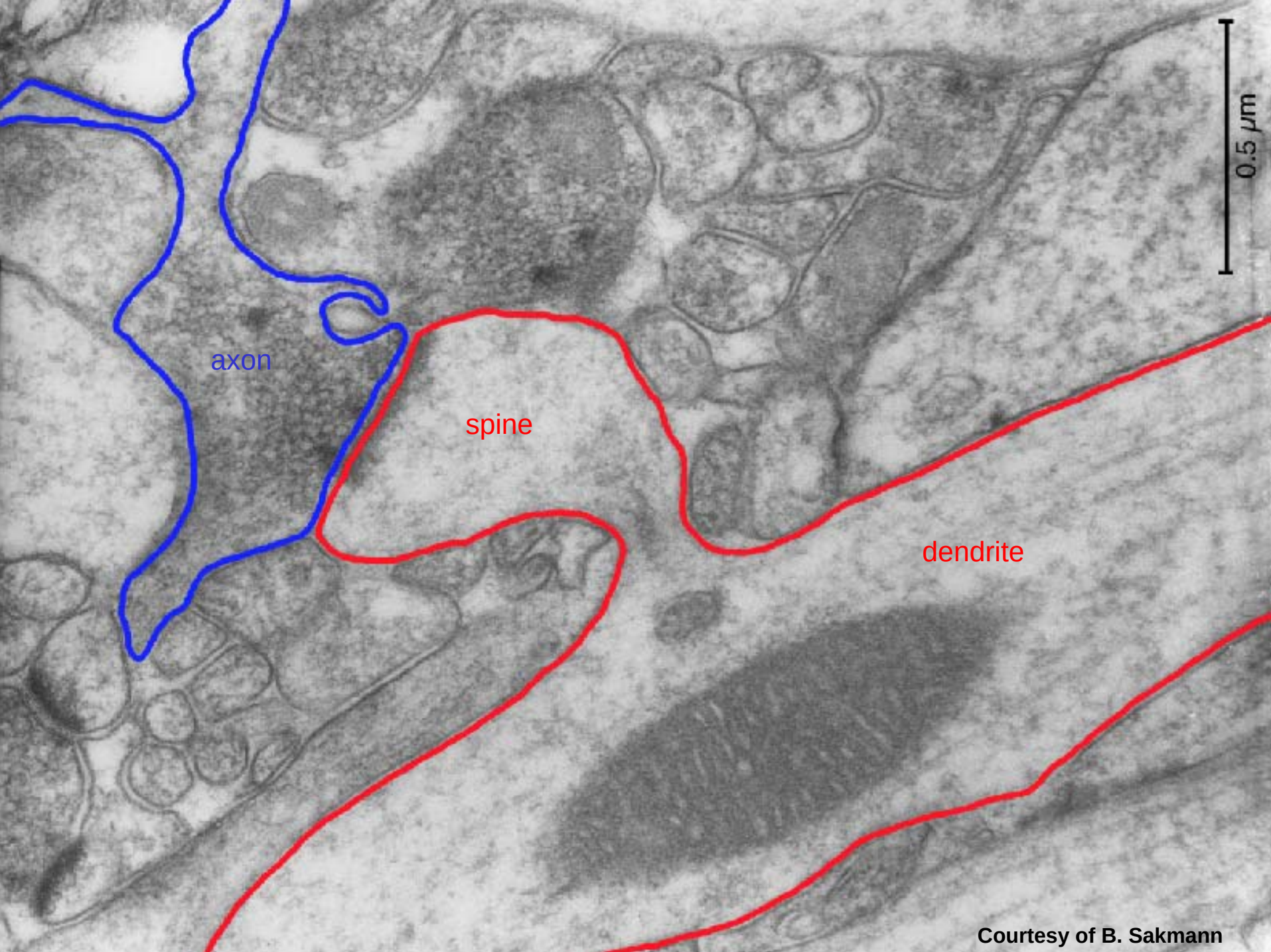

Courtesy of B. Sakmann

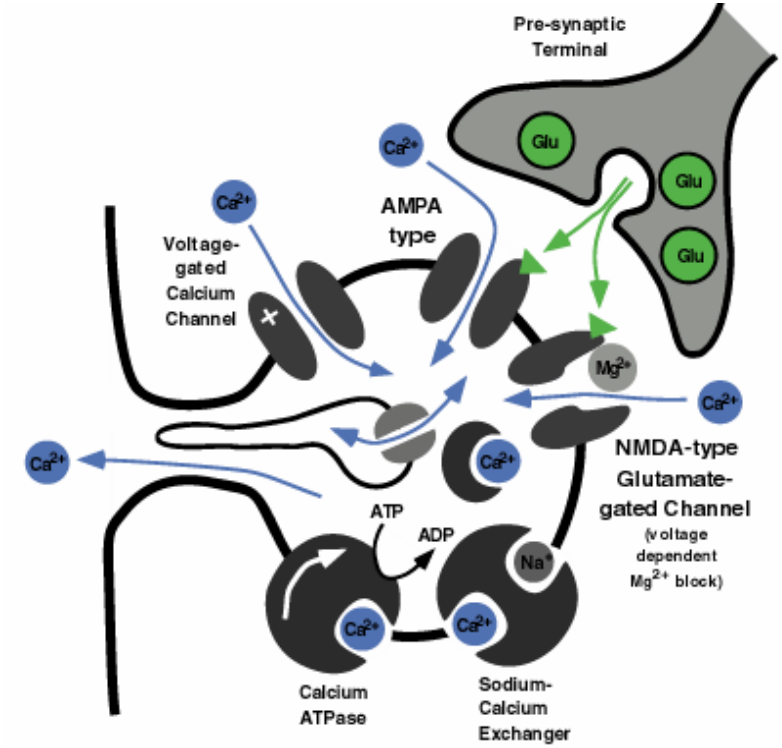
Pre-synaptic
Terminal
Glu
Glu
Glu
Ca2+
Ca2+
AMPA
type
Voltage-
gated
Calcium
Channel
+
Mg2+
Ca2+
NMDA-type
Glutamate-
gated Channel
(voltage
dependent
Mg2+ block)
Ca2+
Ca2+
ATP
ADP
Na+
Ca2+
Ca2+
Calcium
ATPase
Sodium-
Calcium
Exchanger

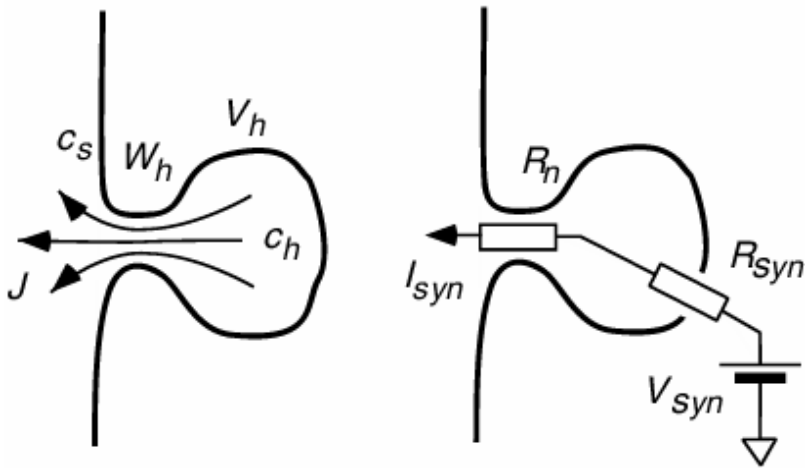
c_s
W_h
V_h
c_h
J
R_n
R_{syn}
I_{syn}
V_{syn}

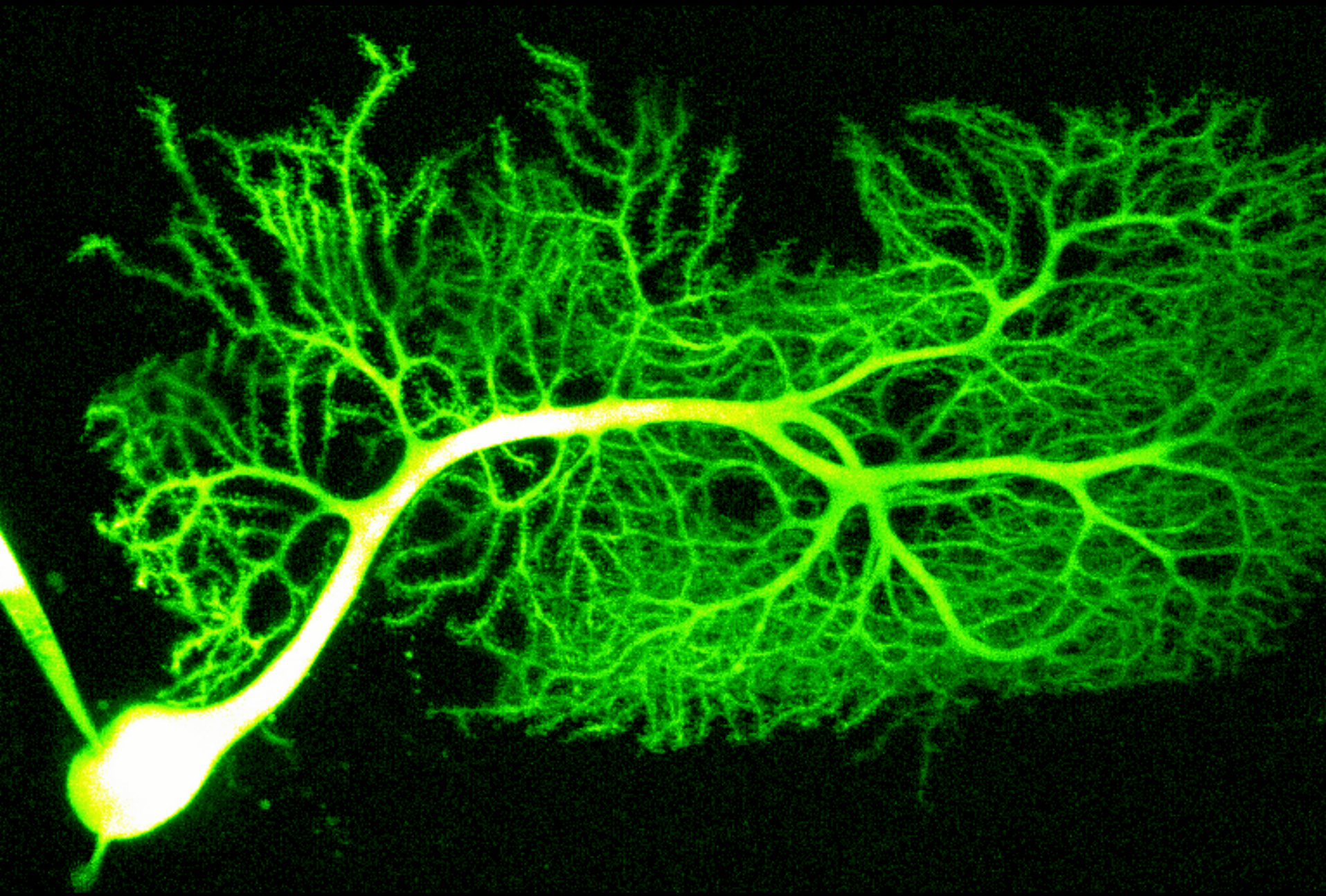

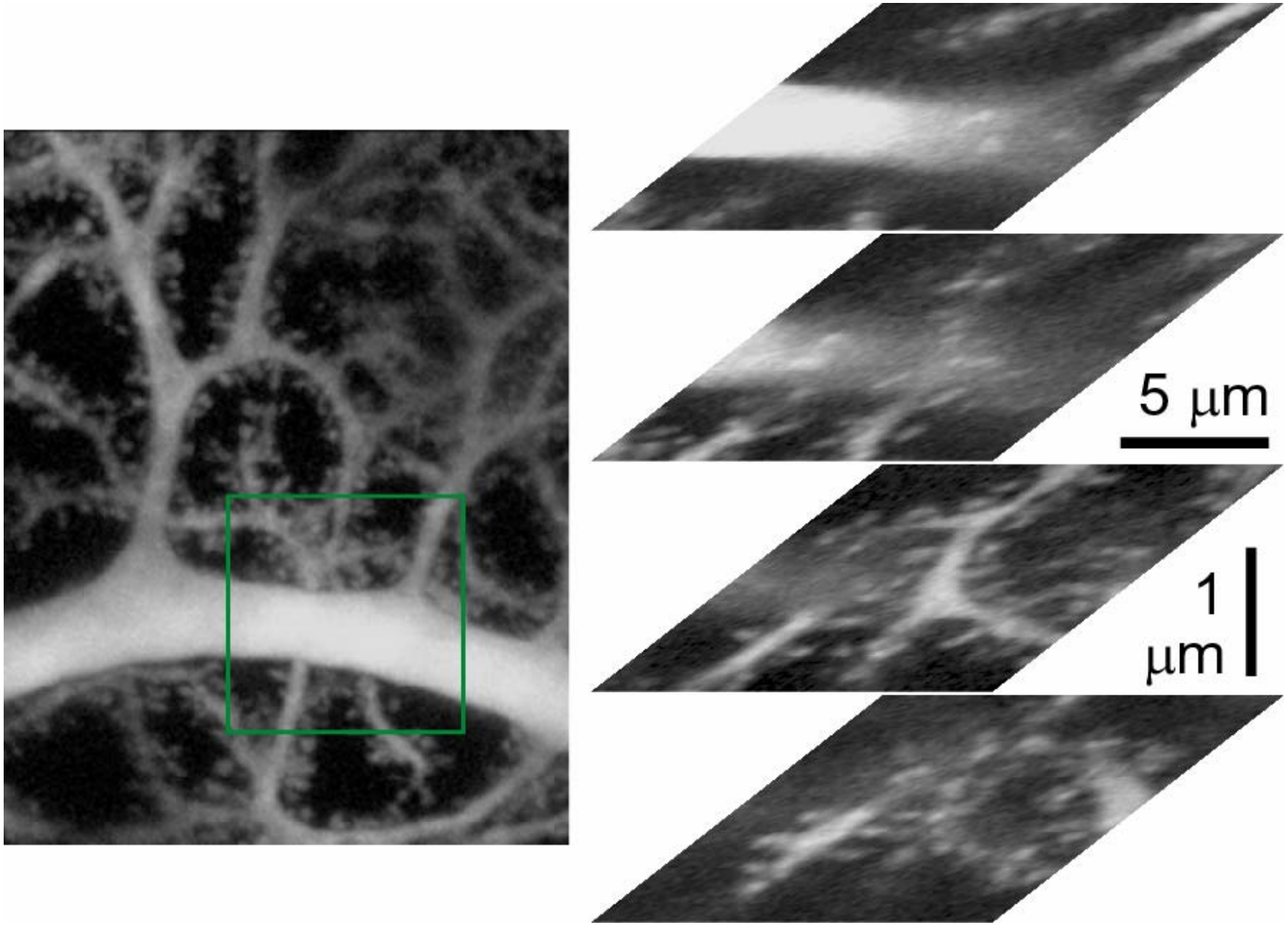
5 µm
1
µm

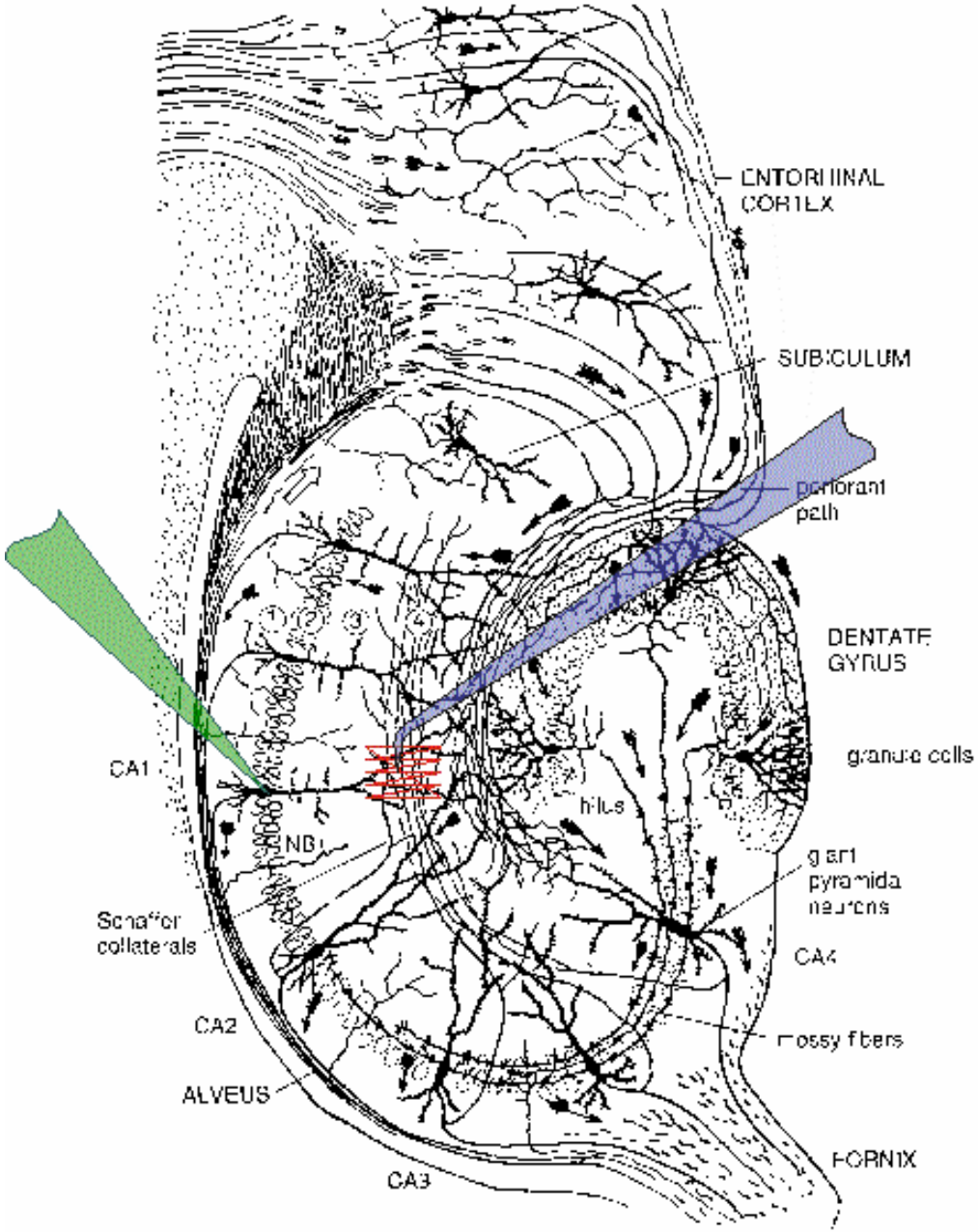
ENTORHINAL CORTEX
SUBICULUM
perforant path
DENTATE GYRUS
granule cells
hilus
CA1
NB
Schaffer collaterals
giant pyramidal neurons
CA4
CA2
mossy fibers
ALVEUS
FORNIX
CA3

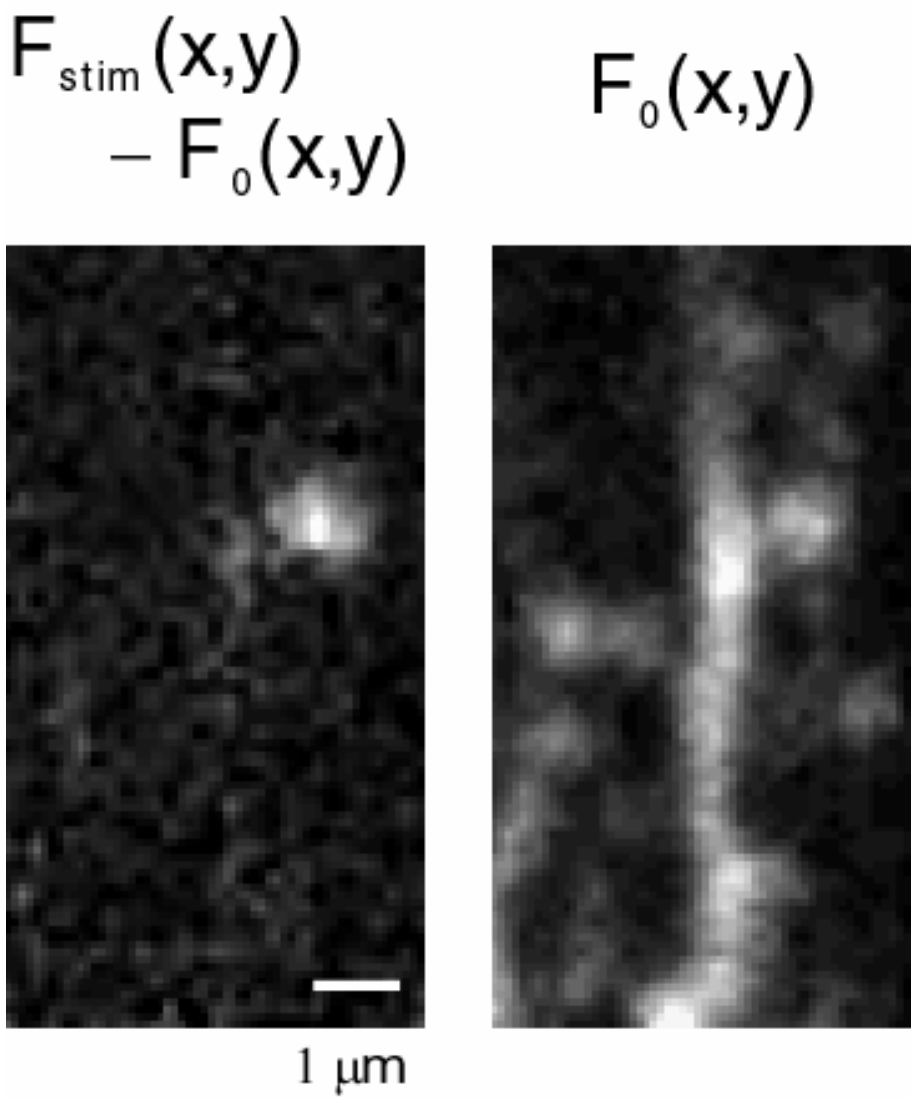
$F_{stim}(x,y) - F_0(x,y)$
$F_0(x,y)$
1 μm

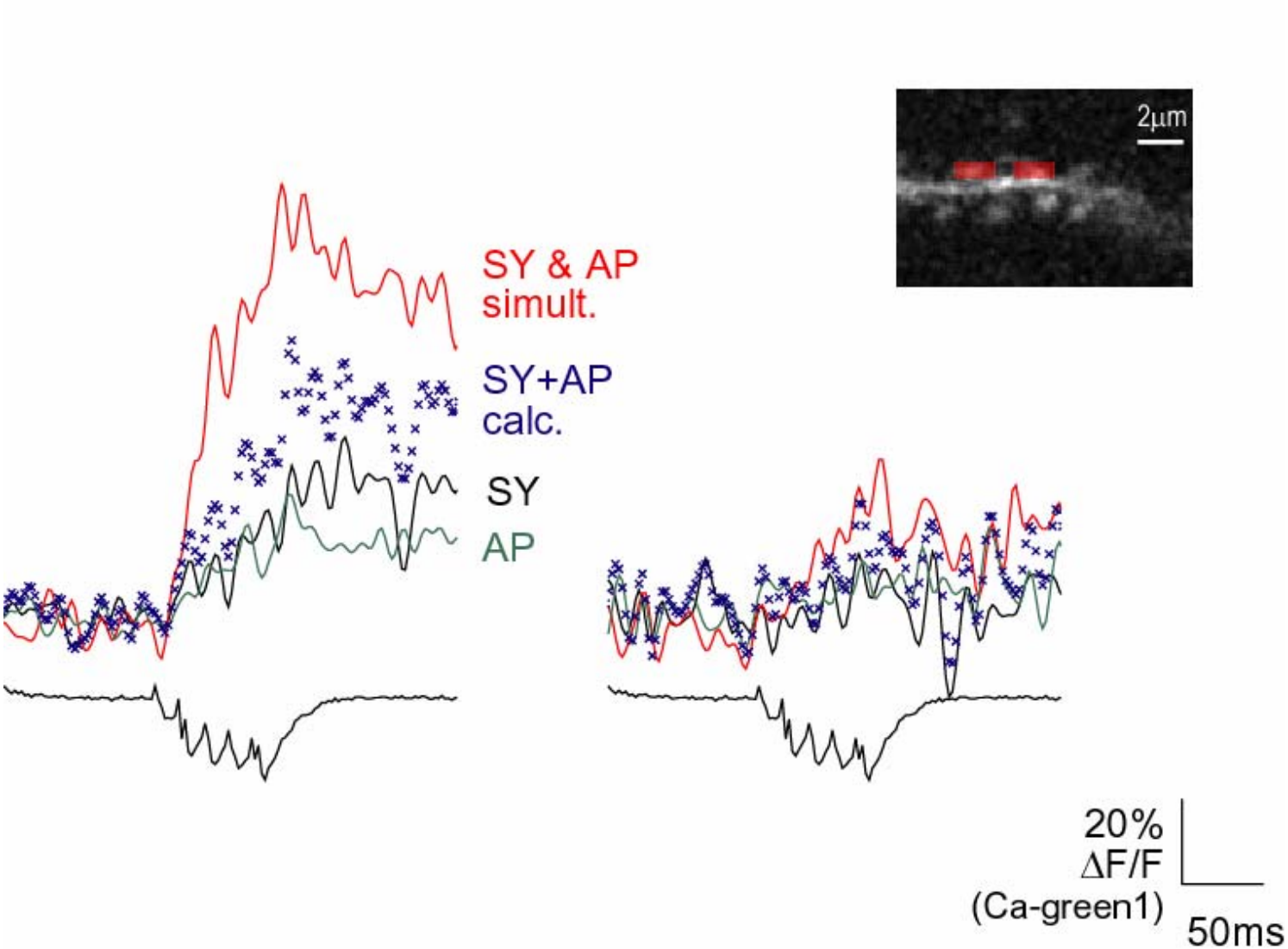

Yuste&Denk, *Nature* **375**, p 682-684 (1995)

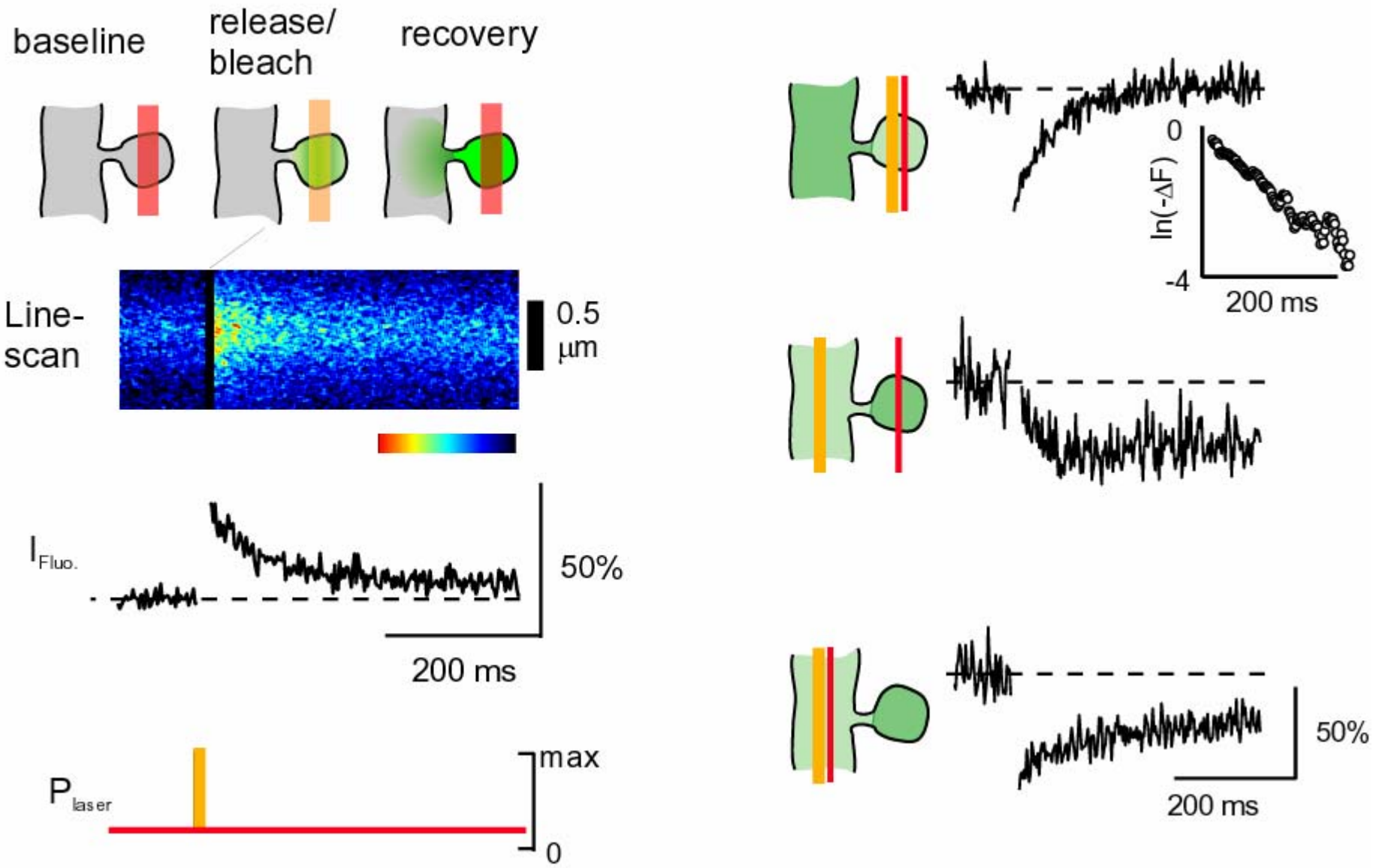
baseline
release/
bleach
recovery
Line-
scan
0.5
µm
$I_{Fluo.}$
50%
200 ms
P_{laser}
max
0
0
ln(-ΔF)
-4
200 ms
50%
200 ms

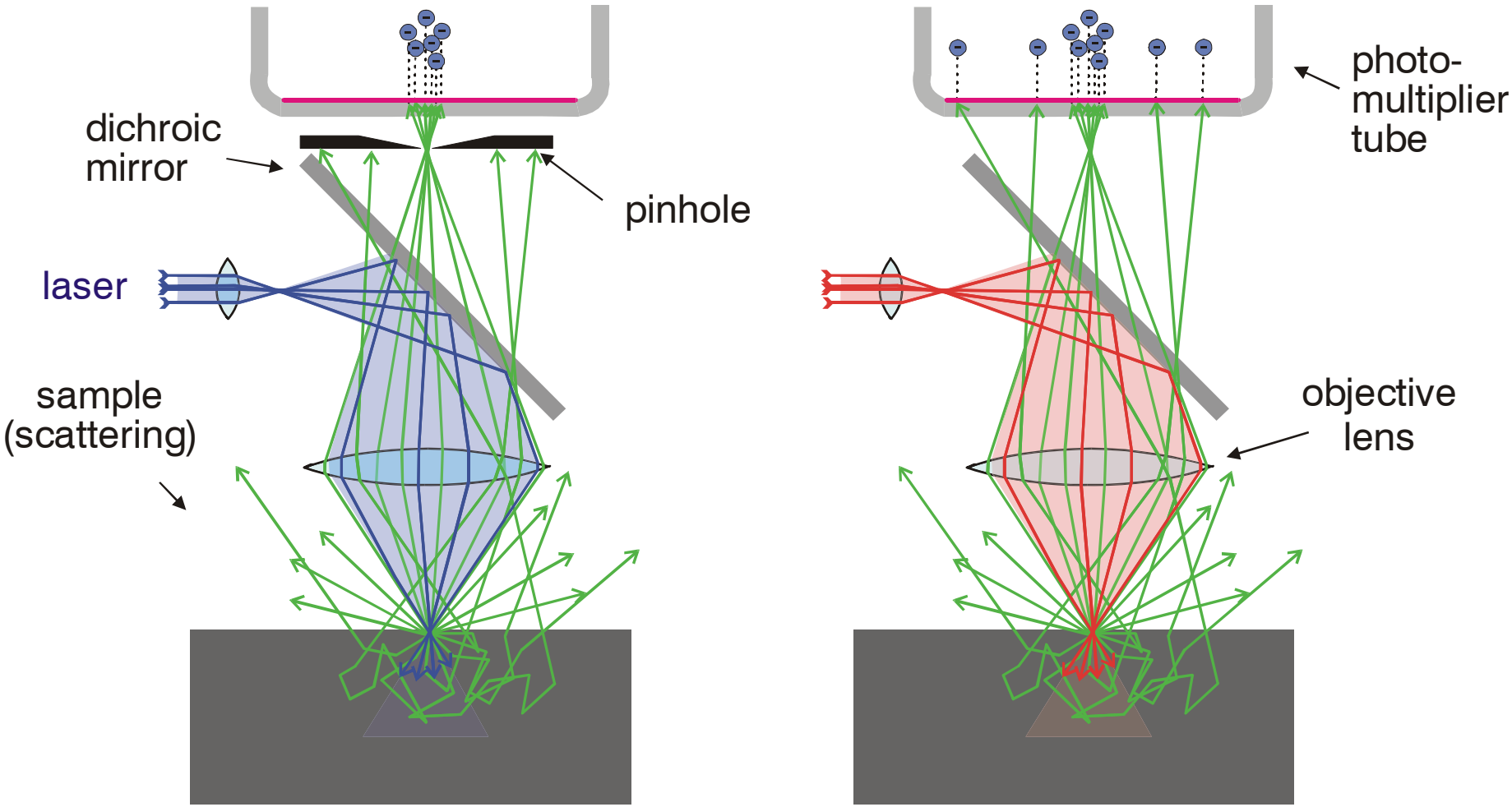
dichroic
mirror
pinhole
laser
sample
(scattering)
photo-
multiplier
tube
objective
lens

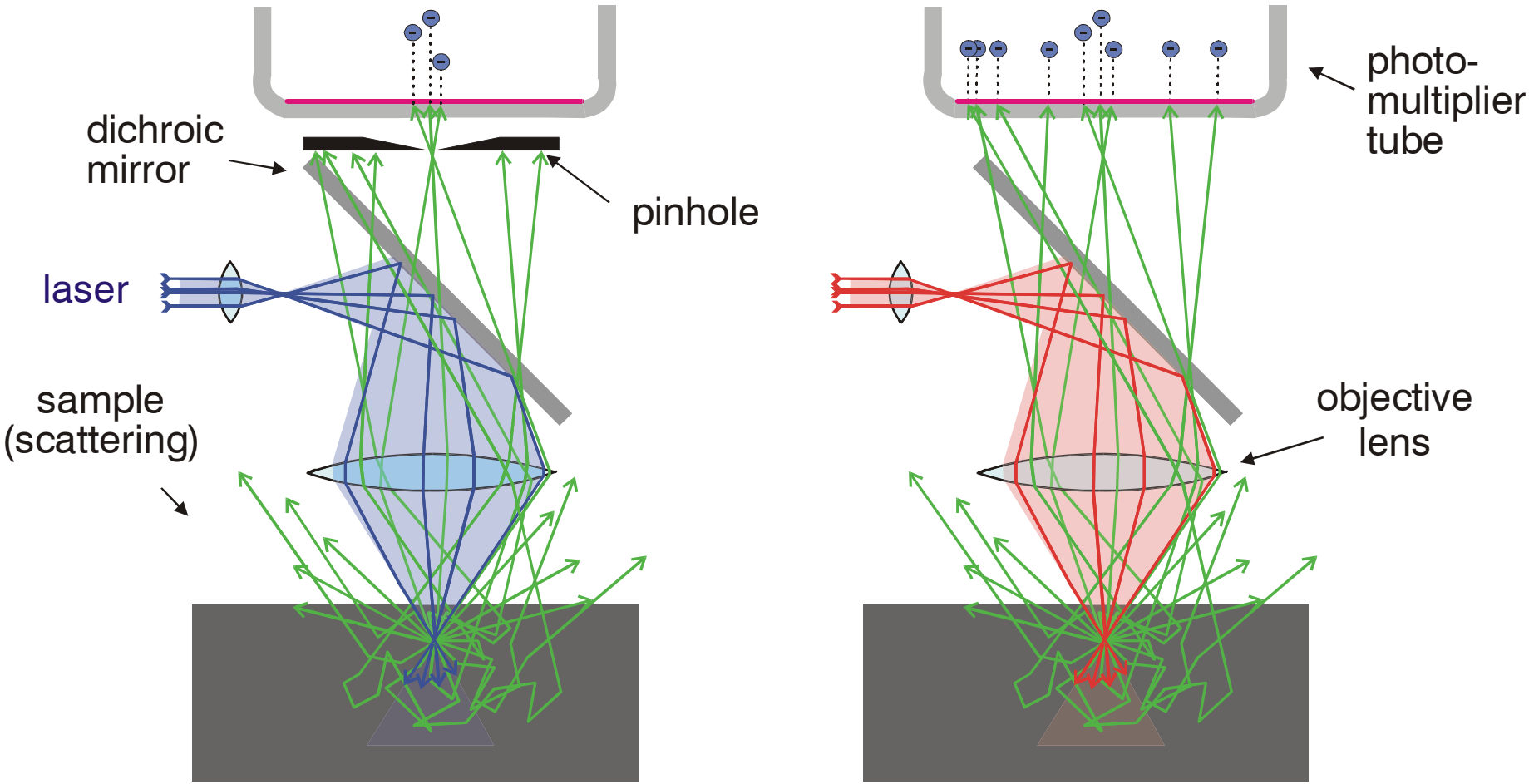
dichroic
mirror
pinhole
laser
sample
(scattering)
photo-
multiplier
tube
objective
lens

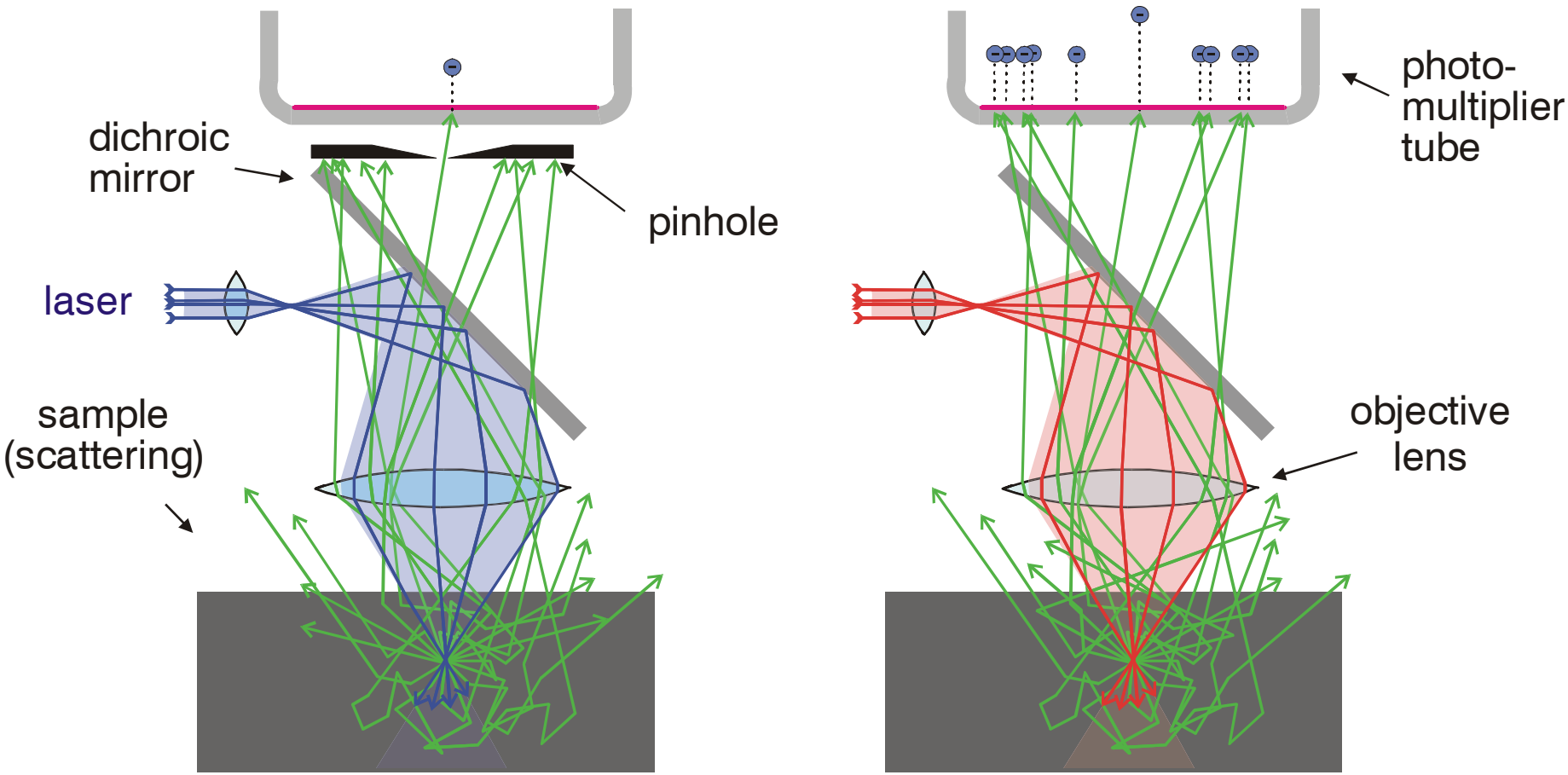
dichroic
mirror
pinhole
laser
sample
(scattering)
photo-
multiplier
tube
objective
lens

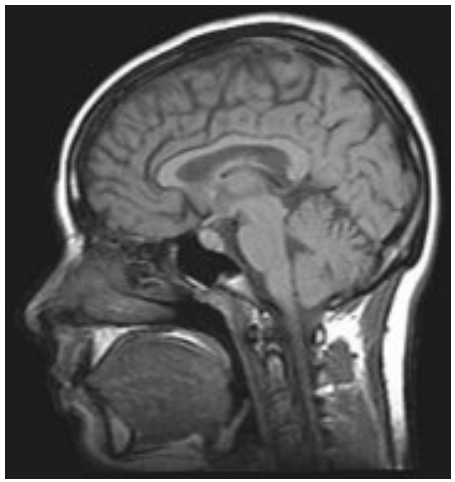

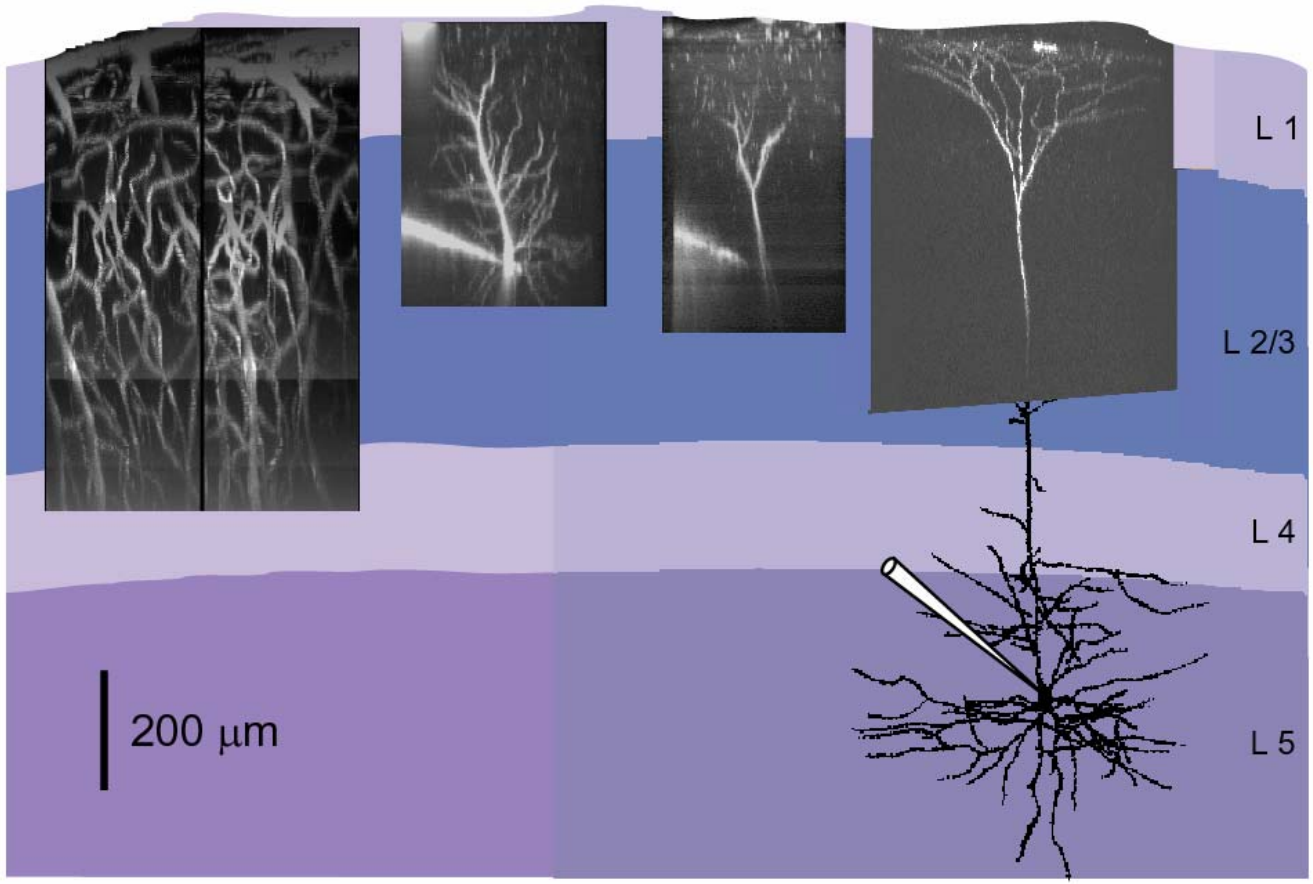
L 1
L 2/3
L 4
L 5
200 μm

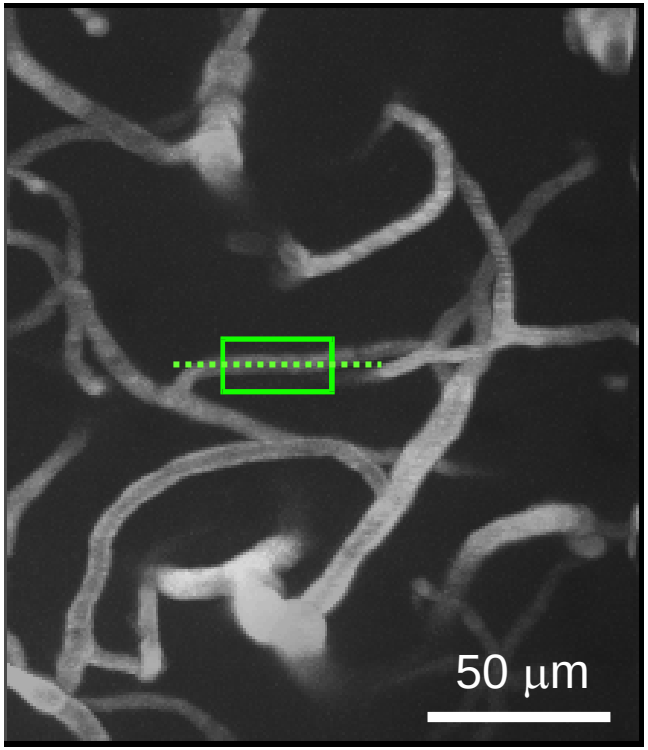

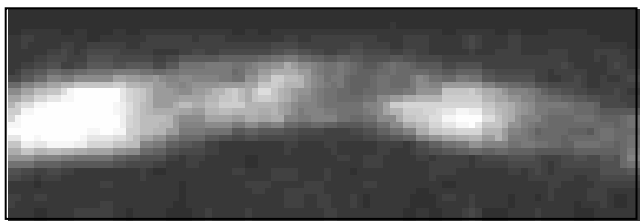

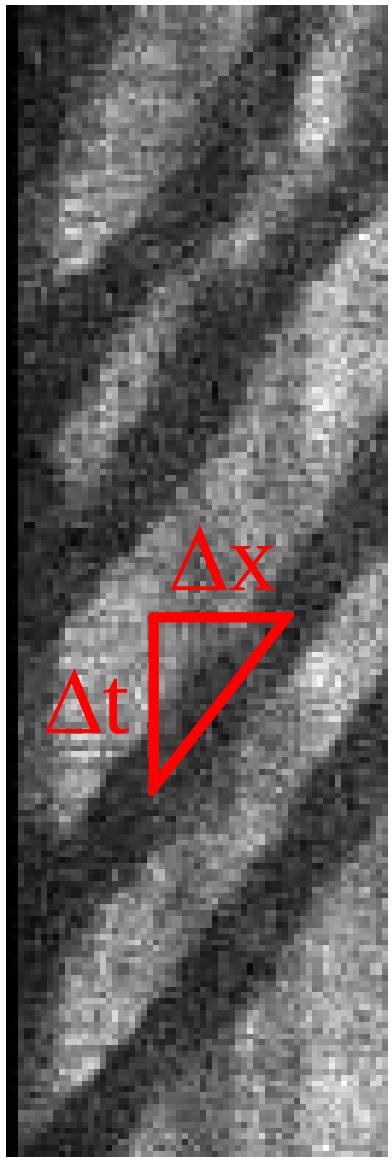

Kleinfeld, Mitra, Helmchen, Denk, *PNAS*, **95**: 15741-15746.

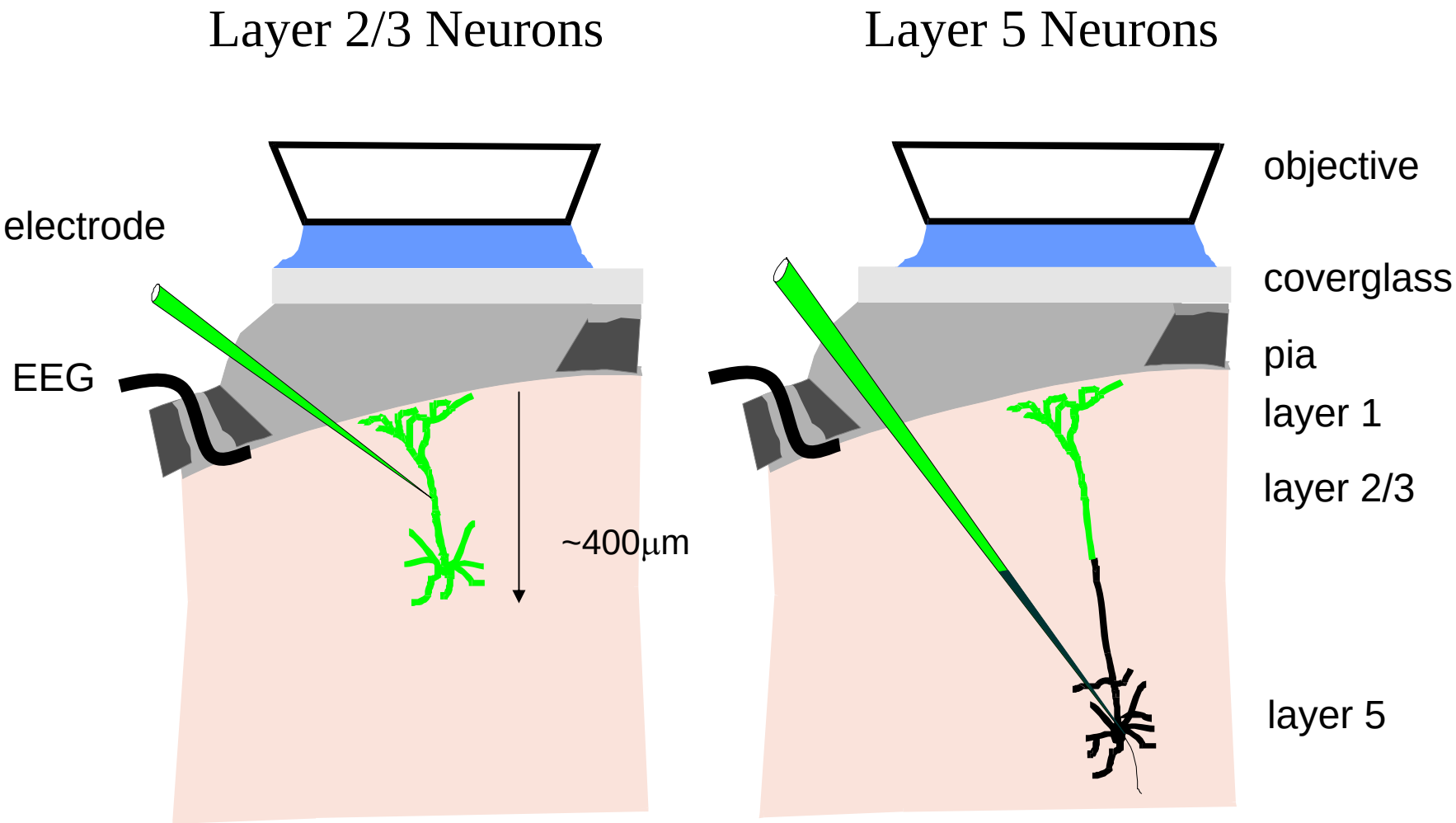
Layer 2/3 Neurons
Layer 5 Neurons
electrode
EEG
~400μm
objective
coverglass
pia
layer 1
layer 2/3
layer 5

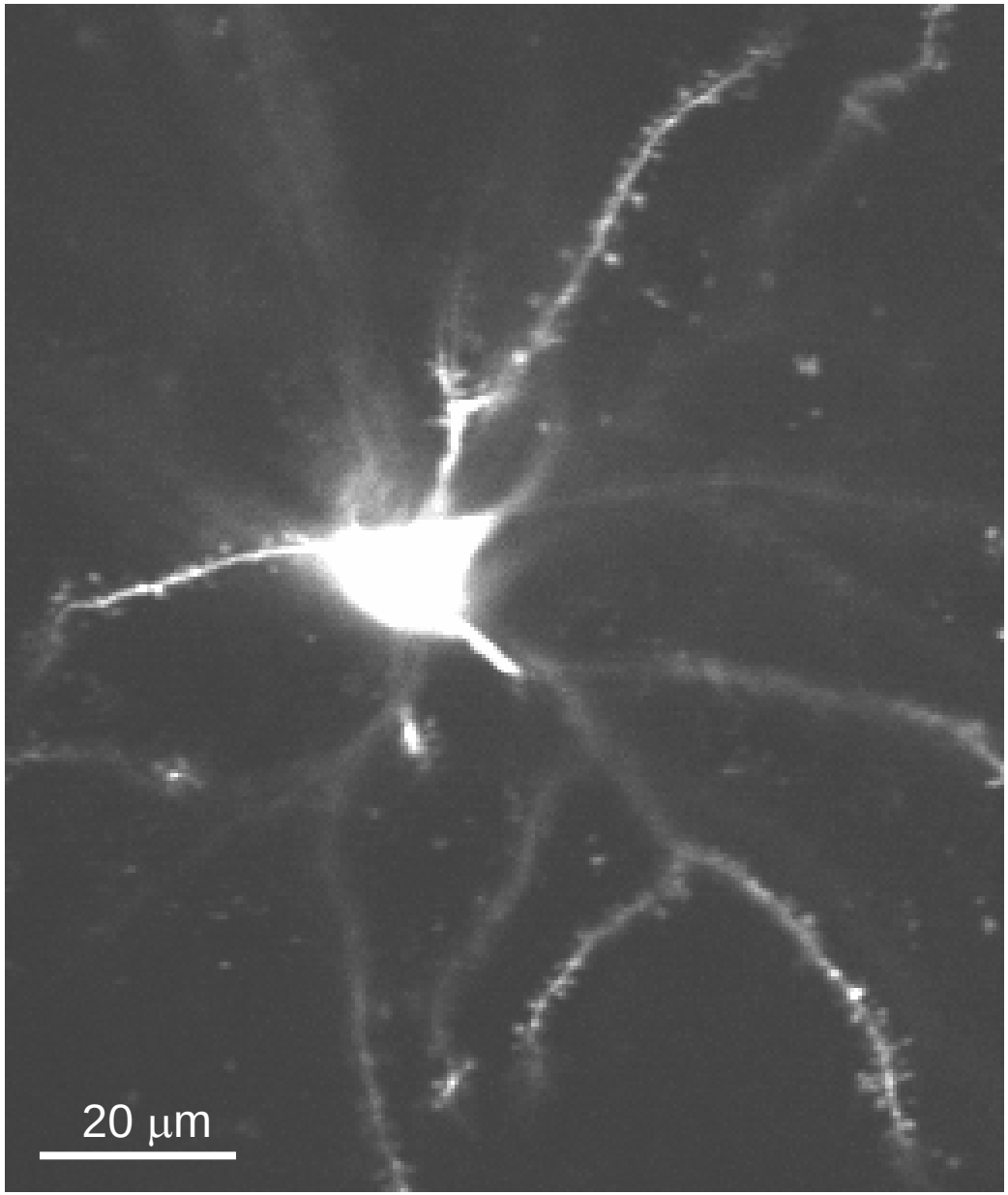
20 μm

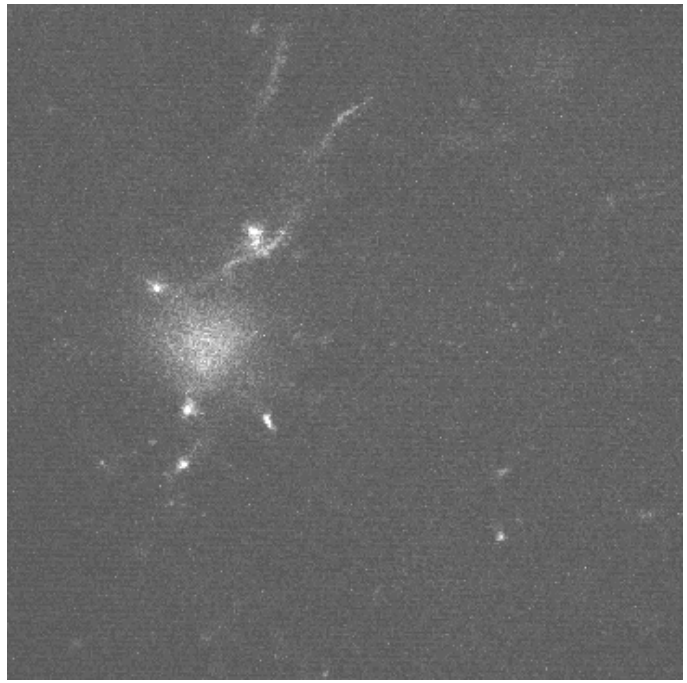

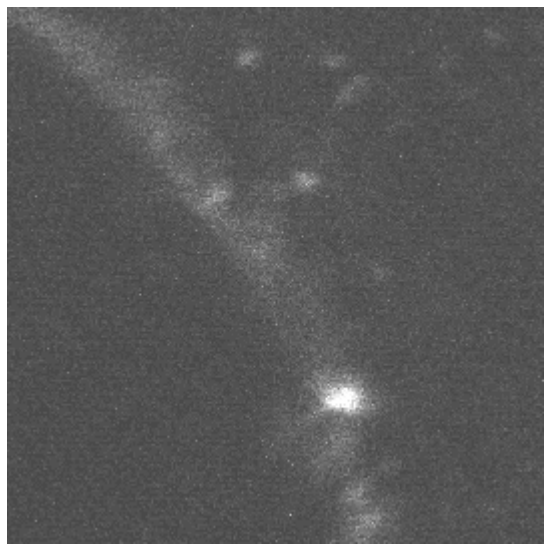

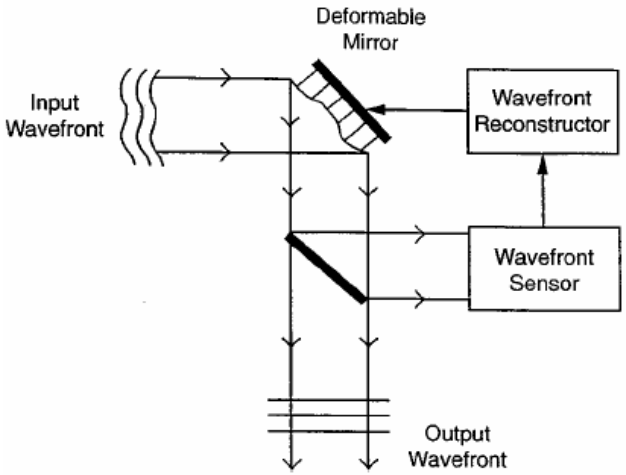

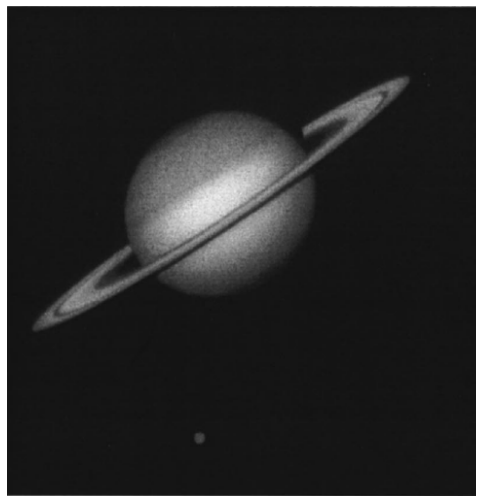

Milonni, P. W. (1999). "Resource letter: AOA-1: Adaptive optics for astronomy." Am. J. of Physics, **67**(6): 476-485.

Marsh, P. N., D. Burns and J. M. Girkin (2003). "Practical implementation of adaptive optics in multiphoton microscopy." Opt Express, **11**(10): 1123-1130.

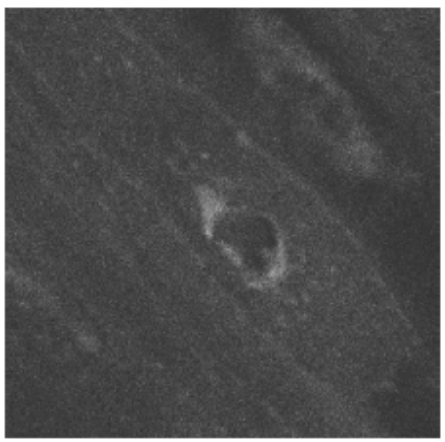

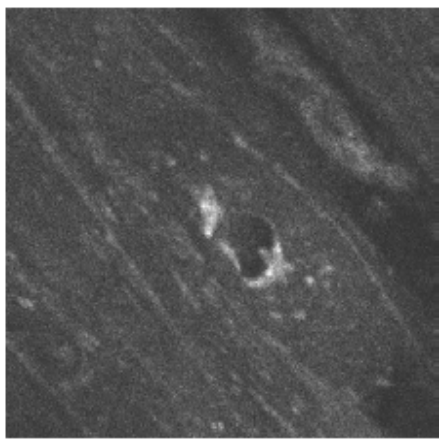

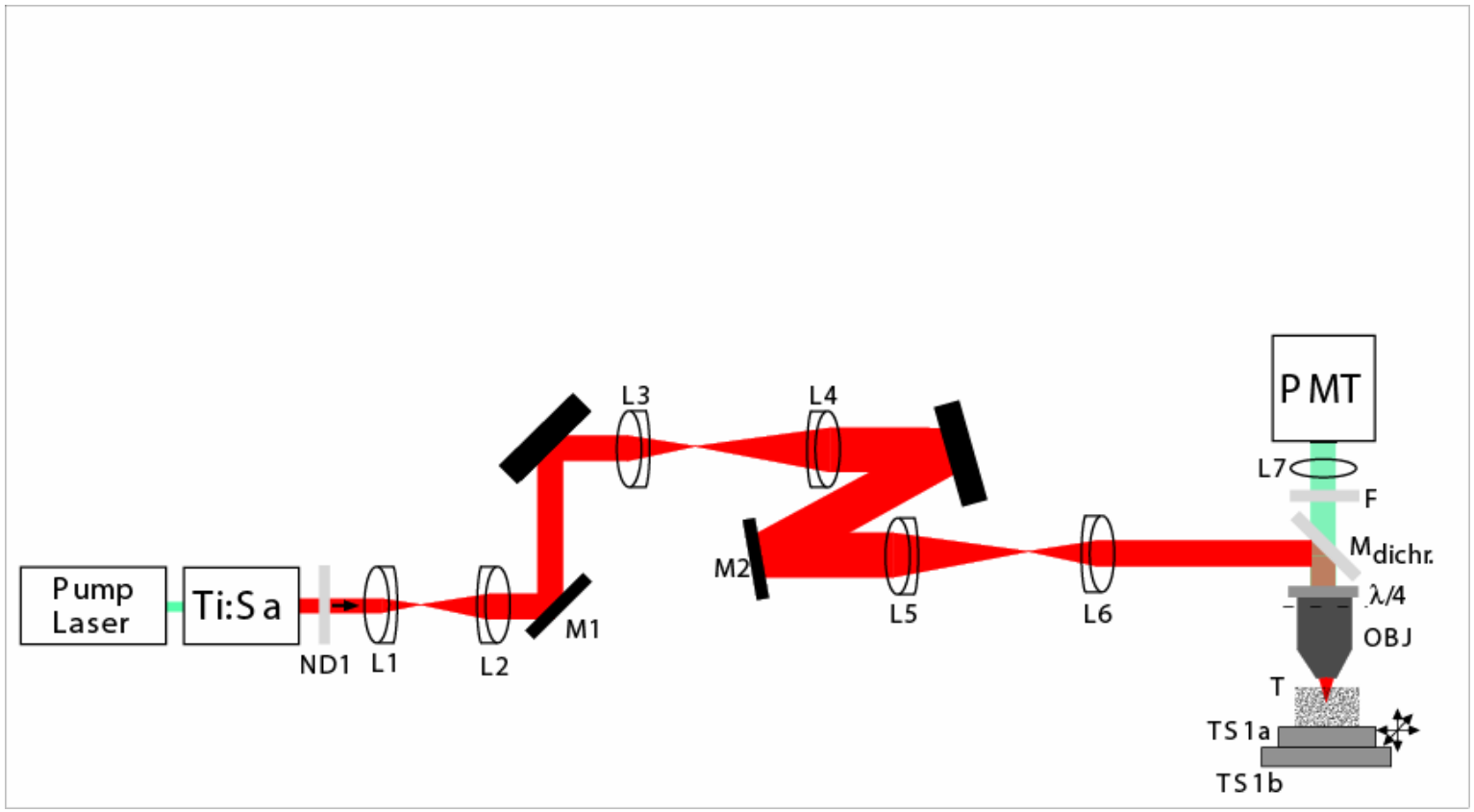
Pump Laser
Ti:S a
ND1
L1
L2
M1
L3
L4
M2
L5
L6
P MT
L7
F
M dichr.
λ/4
OBJ
T
TS 1a
TS 1b

Unscrambling the wavefront: adaptive optics

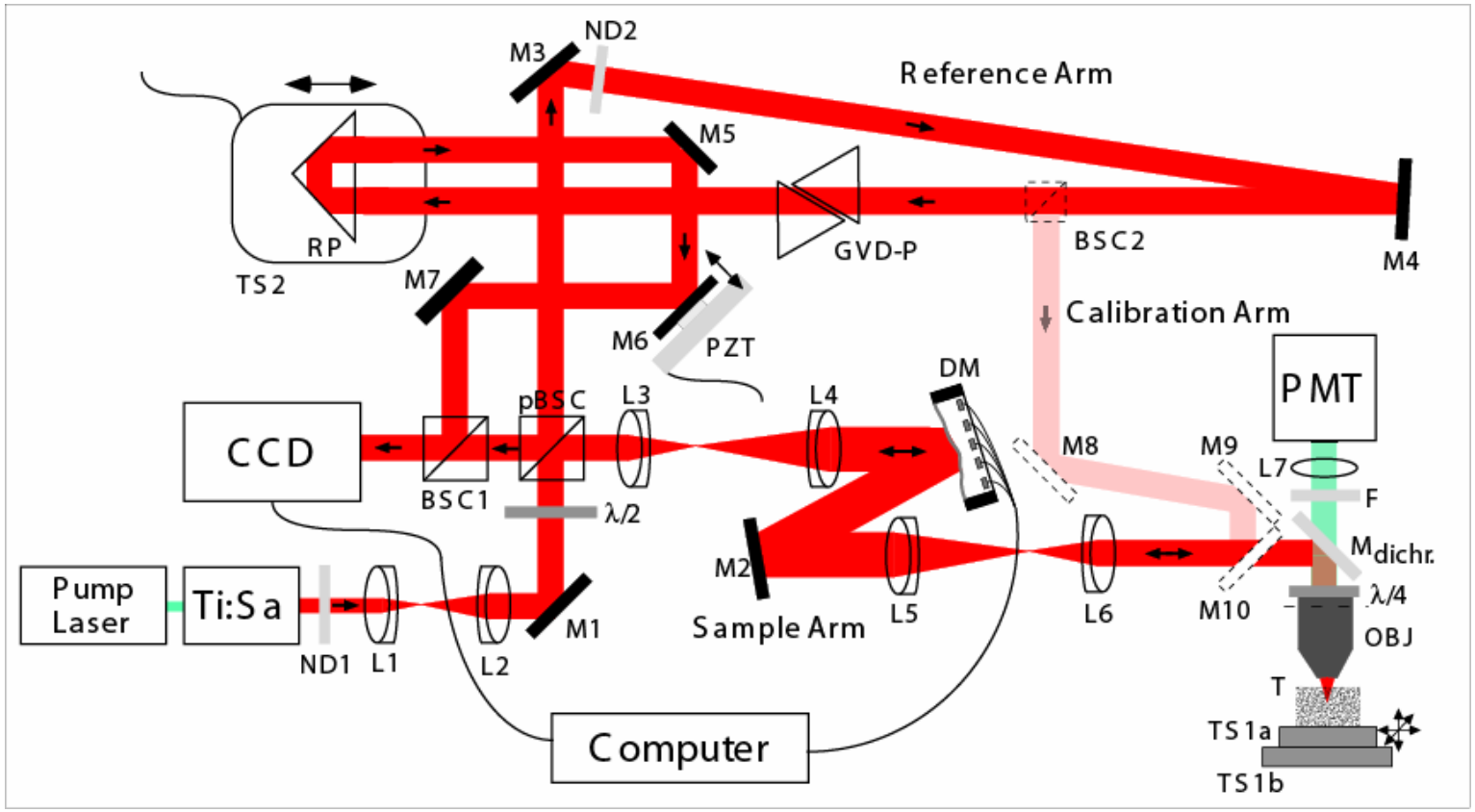

Markus Rueckel, Marcus Feierabend, WD

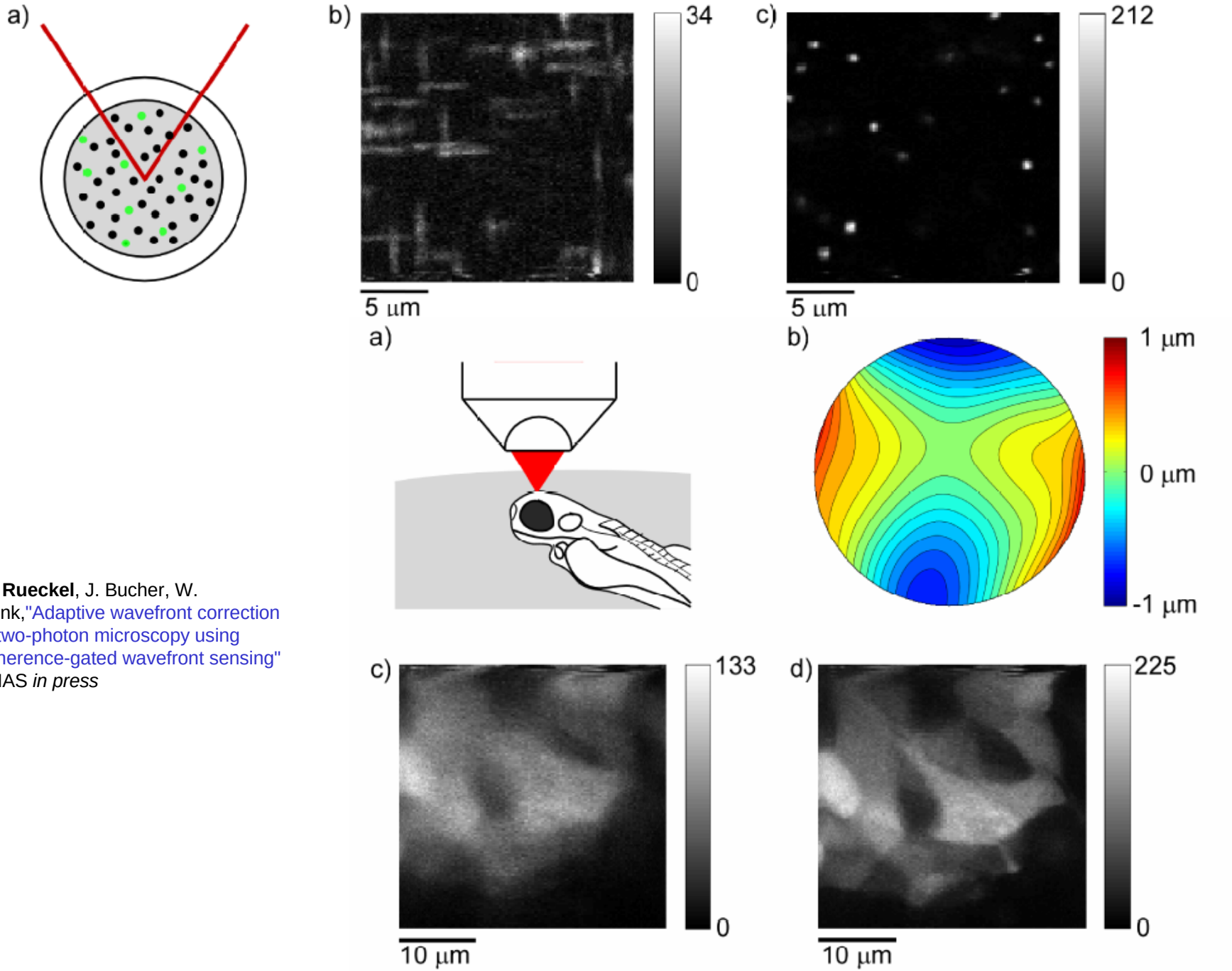

M. Rueckel, J. Bucher, W. Denk,"Adaptive wavefront correction in two-photon microscopy using coherence-gated wavefront sensing" PNAS *in press*

Drosophila embryo expressing tau-mGFP6 pan-neuronally under the control of the ElaV promoter.
Imaged with the Bio-Rad 2-Photon system and a 40X objective.
z-stacks, taken every five minutes over approximately eight hours.
CSH imaging course, Peter van Roessel and WD